



OPEN

Enhanced machining of Al 10%SiC_{micro} 1%SiC_{nano} hybrid composite using rotary tool rotary workpiece EDM with bio dielectrics and treated tools

Umair Arif[✉], Imtiaz Ali Khan & Faisal Hasan

A sustainable approach was proposed to address environmental pollution, carbon footprint and economic efficiency challenges in Electrical Discharge Machining (EDM). This approach involved the use of Bio-dielectric such as biodiesel and Bio fuel (distilled water with 10% ethanol). The EDM process performance was further optimized by experimenting with both electrodes' rotation (i.e., in same direction, opposite direction, no rotation) and the use of treated tools (no treatment, heat treatment, cryogenic treatment). Biodiesel as a bio-dielectric showed promise by delivering the highest Material Removal Rate (MRR) and the lowest Tool Wear Rate (TWR). Bio-fuel (distilled water with 10% ethanol) resulted in the lowest Surface Roughness (SR) and cleaner machined surface with least carbon deposition. Additionally, electrode rotation improved flushing and enhanced performance parameters, with opposite direction rotation yielding the highest MRR and the lowest SR. However, no rotation of electrodes resulted in the lowest TWR. The use of treated tools, specifically heat-treated and cryogenically treated tools, also improved performance and reduced energy consumption, with cryogenic treatment providing the highest MRR, heat treatment giving least SR, and no treatment providing least TWR. Certain interactions between factors significantly impacted performance parameters. Grey relational analysis revealed that using distilled water with 10% ethanol as a dielectric, employing cryogenically treated copper tools, and having no rotation of both electrodes yielded the best performance parameters.

Keywords Rotary tool rotary workpiece EDM, Annealed cu tool, Cryogenically treated tool, Biodiesel, Distilled water with 10% ethanol, Carbon footprint

Electric discharge machining (EDM) process enables the precise cutting of difficult-to-machine materials such as metal matrix composites (MMC's), titanium alloys, tungsten carbide, and nitinol without tool breakage. EDM can be combined with other conventional and non-conventional processes, making it a versatile machining technique. EDM variants such as electric discharge drilling¹, electric discharge milling, electric discharge grinding, electric discharge coating/deposition², Powder mixed EDM (PMEDM)³, Rotary EDM (RT-EDM)⁴, magnetic field assisted EDM⁵, Rotary magnetic field assisted EDM⁶, Ultrasonic assisted EDM (USED⁷), Rotary Ultrasonic assisted EDM⁸, Ultrasonic assisted cryogenically cooled copper electrode EDM (UACEDM)⁹, Abrasive jet assisted EDM (AJEDM)¹⁰, Rotary Abrasive jet-assisted EDM¹¹, and Ultrasonic assisted water jet machining EDM¹² are in practice. During EDM, material is removed through melting and evaporation, and the dielectric fluid then flushes away the debris. Thus, the choice of dielectric has a significant impact on the machined workpiece and process performance¹³. The dielectric fluid allows charged particles to flow to the opposite electrode after ionization in an oxygen-free environment. The viscosity, electrical conductivity, and thermal conductivity of the dielectric fluid determine the initiation of discharge, plasma extension, material degradation, debris clearance via bubble formation¹⁴, and discharge channel reconditioning in EDM¹³. Additionally, the dielectric must have sufficient strength to resist electrostatic fields.

The ISO 14,000 standard places great emphasis on sustainability in all manufacturing processes, including the use of sustainable production techniques that minimize waste, improve environmental performance, and

Department of Mechanical Engineering, Aligarh Muslim University, Aligarh, India. [✉]email: umairarif@zhcet.ac.in

ensure operator safety and health. In the context of EDM, the use of traditional dielectric fluids and high energy consumption pose significant obstacles to achieving sustainability objectives. These fluids, which are typically hydrocarbon-based (such as kerosene), release harmful substances (benzene and polycyclic aromatic hydrocarbons) into the environment in the form of aerosols¹⁵, thereby contributing to respiratory and skin problems as well as environmental pollution¹⁶. In addition, they are non-biodegradable, non-renewable and uneconomical.

Bio-diesel

In the literature, vegetable oils and water-in-oil emulsions have been cited as sustainable alternative dielectric media¹³. The oil extracted from plant seeds is biodegradable, non-toxic, environmentally friendly, and non-hazardous¹⁷. Dastagiri et al.¹⁸ showed that bio dielectrics, such as reused Palmolive oil, are significantly less expensive than commercial EDM oil. Additionally, the usage of bio-dielectric materials increases production efficiency besides being renewable^{19–21}. Therefore, the use of such bio dielectrics should be encouraged in order to make the EDM process more sustainable and environmentally beneficial.

The available literature on vegetable oil-based bio dielectrics for EDM was therefore thoroughly examined. Various bio dielectrics have been used in the literature for electric discharge machining, such as tap water²², neem oil^{23,24}, Jatropha BD^{19–21}, Glycerin-air dielectric²⁵, Polanga¹⁷, Palm oil²⁶, Kusum oil²⁷, Sun flower oil²⁸, canola oil²¹, Pongamia oil²⁹. According to certain studies, Jatropha oil, outperformed kerosene in terms of material removal rate (MRR), surface roughness (SR), and surface hardness^{19–21}. Valaki et al.²⁶ discovered that a bio-dielectric fluid based on palm oil had a 38% higher MRR and nearly the same surface hardness and roughness as kerosene oil. Mishra and Routara¹⁷ found that Polanga bio-dielectric oil enhances mean MRR by 0.86 times, improves surface finish by 16.64%, increases surface stiffness by 6.46%, and emits 17.33% less aerosol when compared to standard hydrocarbon dielectrics. According to Bajaj et al.²⁷, Multiwall carbon nano tube (MWCNT) mixed in Kusum oil using rotary EDM, resulted in about 57.14% greater MRR and 54.57% lower surface roughness. Further, Das et al.³⁰ examined 3 bio dielectrics and discovered that compared to kerosene oil, Neem oil-based bio-dielectric created 18% extra overcut and 40% further tapper cut, Canola oil-based bio-dielectric generates 12% less surface roughness, and Jatropha oil-based bio-dielectric generates 15% more MRR. Singh et al.³¹ demonstrated that Pongamia oil had superior MRR, electrode wear ratio (EWR), and surface roughness compared to Jatropha oil, whereas kerosene oil had the weakest performance metrics among the three dielectrics. It can be concluded that when compared to conventional dielectrics, virtually all bio dielectrics demonstrated improved machine characteristics. However, Khan et al.³² have reported that amongst all bio-oils, Waste Vegetable Oil (WVO) has the highest impact index of sustainability. WVO is the cheapest of all vegetable oils, has the highest conversion ratio and has the most economical process³³. Hence Biodiesel based on waste vegetable oil was used as one of the bio dielectrics.

Bio-fuel

Literature also showed that using distilled water as dielectric³⁴, resulted in superior machining conditions compared to hydrocarbon oil with a Ti-6Al-4 V workpiece and copper electrode. Similarly using Commercial water-based fluids, such as Elbolub (manufactured by Elotherm, Germany)³⁵ resulted in 2–3 times higher MRR than conventional oil. Researcher have also found that adding organic compounds such as polyethylene glycol 600³⁶, glycerine in high concentration³⁷, urea³⁸ in water also gave better results than convention dielectrics. However, to the best of authors knowledge, the literature does not reveal any investigation into the using distilled water mixed with certain percentage of ethanol as bio-dielectric.

The reason for using ethanol is that, Ethanol is one of the principal biofuels which is produced by fermentation of sugars or via Petro-chemical process. India, Brazil, and Indonesia are among few countries that produce ethanol from fermentation of sugar thereby making ethanol production as renewable with no significant emission of greenhouse gases (mainly CO₂) and highly positive energy balance³⁹. Indian government is highly focussed on increasing the production of ethanol from sugarcane as part of plan to introduce biofuels to the market to attain global decarbonization and net zero emissions as per The National policy on Biofuels 2018⁴⁰. Hence the government has taken all incentives to increase the supply of ethanol which is 332 crore litres in 2020–21 and is projected to 1016 crore litres in 2025–26. Uttar Pradesh is leading in the production of bio-Ethanol. Tsiropoulos et al.⁴¹ showed that compared to Brazilian ethanol, Indian ethanol causes lower or comparable greenhouse gas emissions (0.09–0.64 kg CO₂eq/kg ethanol_{IN}, 0.46–0.63 kgCO₂eq/kg ethanol_{BR}), non-renewable energy use (–0.3–6.3 MJ/kg ethanol_{IN}, 1–4 MJ/kg ethanol_{BR}), human health impacts (3.6–10–6 ALY/kg ethanol_{IN}, 4–10–6 DALY/kg ethanol_{BR}) and ecosystem impairment (2.5 PDF·m²·year/kg ethanol_{IN}, 3.3 PDF·m²·year/kg ethanol_{BR}) specially in the state of UP. In light of the enormous environmental benefits of ethanol and the Indian government's plans to dramatically boost its production in the near future, it would be prudent to employ it as a bio dielectric in EDM.

However it was observed that using pure Ethanol as bio-dielectric in EDM⁴² gave second best results when compared with Deionized water and kerosene oil with best results obtained by deionized water dielectric. The reason being pure ethanol (CH₃CH₂OH) has 51.7% carbon weight fraction, therefore, when a molecule of ethanol decomposes, it produces carbon content. The interelectrode gets contaminated by carbon which leads to short circuit and reduced machining efficiency. Besides pure ethanol has high evaporation rate. However distilled water is one dielectric fluid which does not contain any carbon⁴². Hence a solution of distilled water containing 10% ethanol was used as bio-dielectric. This solution resulted in the carbon percent of 5.17%. The viscosity and density being an important properties of dielectric¹³ were also largest at this ratio⁴³.

Energy consumption

Regarding energy consumption, Gutowski et al.⁴⁴ have shown that EDM requires high specific energy, approximately 30–50 times greater than that required by conventional machining processes, and offers slower machining

rates, approximately 50–60 times slower than conventional processes. However, by optimizing the performance parameters, machining rates can be improved and energy consumption can be reduced. One such way is by rotating both electrodes of EDM which results in improved flushing conditions thereby improved performance parameters⁴⁵. However, it was observed in authors previous work, rotating both electrodes in opposite direction as same speed resulted in reduced performance parameters due to reduced flushing⁴⁶. Hence it was decided to further examine the results of performance parameters when both electrodes were rotated in same direction, opposite direction and no rotation. Another way of optimizing performance parameters is the use of treated tool in place of normal tool. The use of cryogenically cooled tool electrodes^{47–49} resulted in higher MRR, lower electrode wear, better machining accuracy, and higher corner size machining accuracy than conventional EDM. Beside in the last work it was visible that at higher rpm of workpiece and tool rotation, rounding of the tool edges was observed which resulted in reduced machine accuracy⁴⁶. Hence in order to improve tool wear resistance, strength, life and thermal stability it was decided to use a heat treated tool (HTT) by annealing and cryogenic treated tool (CTT) by cooling it in liquid nitrogen⁵⁰.

Hence in order to shift EDM towards greener and more sustainable manufacturing process, it was decided to use bio-diesel, distilled water and 10% ethanol solution as bio-dielectric and treated copper tool as well as rotation of both electrodes. The novelty of work lies in the use of distilled water and 10% ethanol solution as bio-dielectric, heat treated copper tool and both electrodes rotation. Table 1 shows very limited literature has machined hybrid composites using EDM. Hence machining Al-10%SiC_{micro}-1%SiC_{nano} workpiece with above set of process parameters also brings in some sort of novelty.

Objective

To investigate the impact of bio-dielectrics on the Al-10%SiC_{micro}-1%SiC_{nano} hybrid composite using RT-RW-EDM along with treated copper tools.

Methodology

Al-10%SiC_{micro}-1%SiC_{nano} hybrid MMC was used as workpiece. 27 samples of workpiece were prepared by powder metallurgy. Al micro powder and SiC micro powder were procured from CDH company. SiC nano powder was procured from GLR company. Initially 40 gm of Al powder was taken. Then SiC micro powder and SiC nano powder were taken as 10% and 1% of the total composite weight and mixed with Al powder in centrifugal ball milling machine (FRITSCH, Germany) at 700 rpm for 20 min with powder to ball ratio as 1:2. 1.5 gm of the mixed powder was taken and compacted in hydraulic press at 400 mpa. The same was sintered at 600 °C with a holding time of 45 min in an inert gas environment. The manufactured tablets as shown in Fig. 1.

Hybrid composites machined by EDM	Authors
Al-5.3% Cu-SiC-Al ₂ O ₃	⁵¹
LM-6 alloy-2wt.% SiC + 4wt.% B ₄ C, LM-6 alloy-4wt.% SiC + 2wt.% B ₄ C	⁵²
Al 4032-6% TiC-2% h-BN	⁵³
LM13 Al alloy-5wt% TiC-10wt% ZrB ₂	⁵⁴
Al 7075-TiC-B ₄ C	⁵⁵
AlSi10Mg alloy-3 wt% graphite-9 wt% Al ₂ O ₃	⁵⁶
A713-2% Bamboo Leaf Ash -2% Al ₂ O ₃ , A713-4% Bamboo Leaf Ash -2% Al ₂ O ₃ , A713-2% Bamboo Leaf Ash -4% Al ₂ O ₃	⁵⁷
Al 2024-6% TiB ₂ -12% B ₄ C	⁵⁸
Al-10% wt SiC-5% wt B ₄ C-1% wt Mg	⁵⁹

Table 1. Shows recent literature that has machined hybrid composites using EDM.



Fig. 1. Shows Al-10%SiC_{micro}-1%SiC_{nano} MMC.

Biodiesel was trans-esterified from waste cooking oil (usually mustard oil) using methanol and KOH⁶⁰. Waste cooking oil was collected from various large gatherings functions such as marriage functions where huge amount of cooking oil is left as waste. Hence collecting waste cooking oil was free of cost. Waste cooking oil was then heated to about 50 °C and 8 L of methanol, 400 gm of KOH were added. The temperature of mixture was maintained for 1 h to obtain 40 L of biodiesel. Similarly, 40 L of distilled water was taken and 4 L of ethanol was purchased from chemical shop and mixed to obtain distilled water -10%ethanol bio dielectric. Table 2 presents the cost analysis of all the three dielectrics used in the study.

Three copper tools were machined with diameter of 8 mm. one copper tool was kept as it is ie non treated tool (NTT). Another copper tool was heat treated (HTT) to 600 °C with a holding time of 30 min and cooled in furnace (annealed). Same was done to third tool along with cryogenic treatment (CTT) at -196 °C for 24 h by putting it in liquid nitrogen container as shown in Fig. 2. The same tool was then tempered at 200 °C for 2 h. The experiments were carried out using an ISO pulse generator EDM system shown in Fig. 3.

	EDM oil	Biodiesel	Bio-Fuel
Cost/ltr	125rs/litre	Waste vegetable oil—free of cost 8 l of Methanol—224rs 400 gm -Koh—280rs Biodiesel—15rs/litre	4 L—ethanol-260rs 40 L of distilled water- free of cost Bio-Fuel-7rs/litre

Table 2. Depicts the cost of all three dielectrics.



Three tool- NTT, HTT, CTT.



Heating furnace used to heat tool at 600 degree Celsius.



Tool dipped in liquid nitrogen container for 24 hrs.

Fig. 2. Shows non treated cu tool, heat treated cu tool and cryogenic treated cu tool.



Fig. 3. Depicts the Electric discharge machine used in the experiment.

Experimental setup

The modified variant of EDM namely RT-RW-EDM comprised of rotary tool setup and rotary workpiece set up as shown in Fig. 4. The rotary tool setup was designed using electric motor/motor drive, pulley and belt drive, tool holder and steel platform with bearing fixed in between the latter two. The point of contacts of motor drive to steel platform were insulated to prevent flow of charges to the motor from cathodic tool. The same is shown in Fig. 5. The rotary workpiece setup was designed using electric motor/ motor drive, aluminium workpiece holder and chain and socket placed connecting them along with three ball bearings holding the workpiece and motor shaft in place. They were placed on a wooden platform to avoid the transfer of charges to motor. The workpiece holder was connected to anodic base of EDM tank with the help of a wire. The workpiece rotary setup is shown in detail in Fig. 6. The EDM dielectric storage tank was replaced with smaller size tank with a desert cooler pump for pumping the dielectric in the machining area Fig. 7. The distilled water with 10% ethanol mixture and biodiesel prepared from waste vegetable oil were placed in the smaller tank and pump into the machining area using desert cooler pump. The rotation direction of both electrodes was varied as same direction of both, opposite direction of both and no rotation of both. The non-treated, heat treated and cryogenic treated copper tools were used.

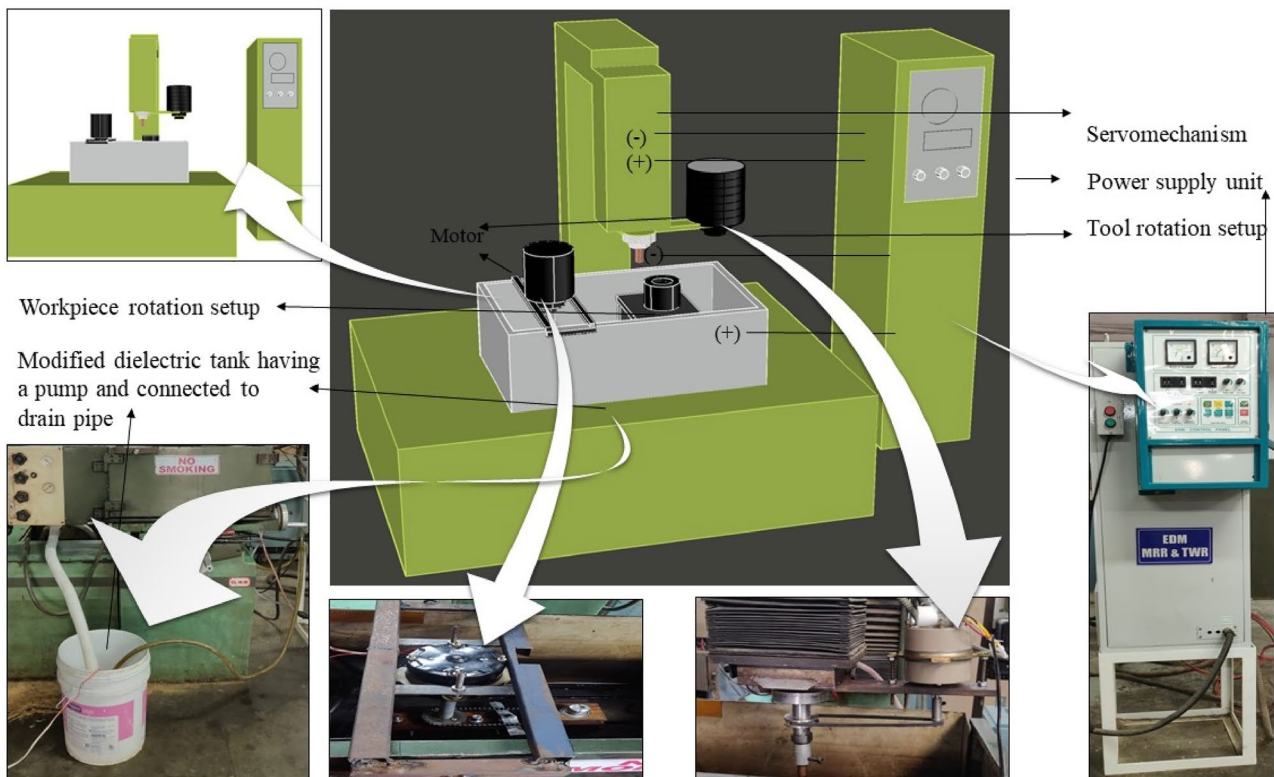


Fig. 4. Shows the RT-RW-EDM.

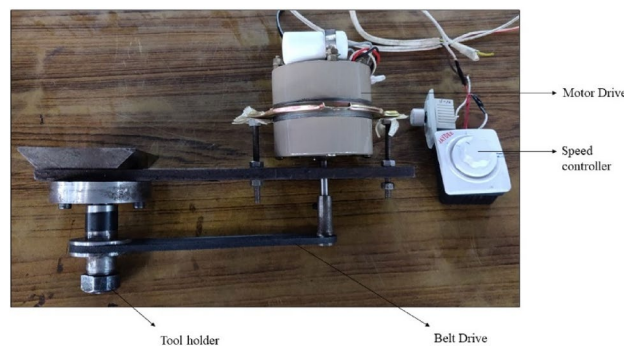


Fig. 5. Shows rotary tool setup used in RT-RW-EDM.

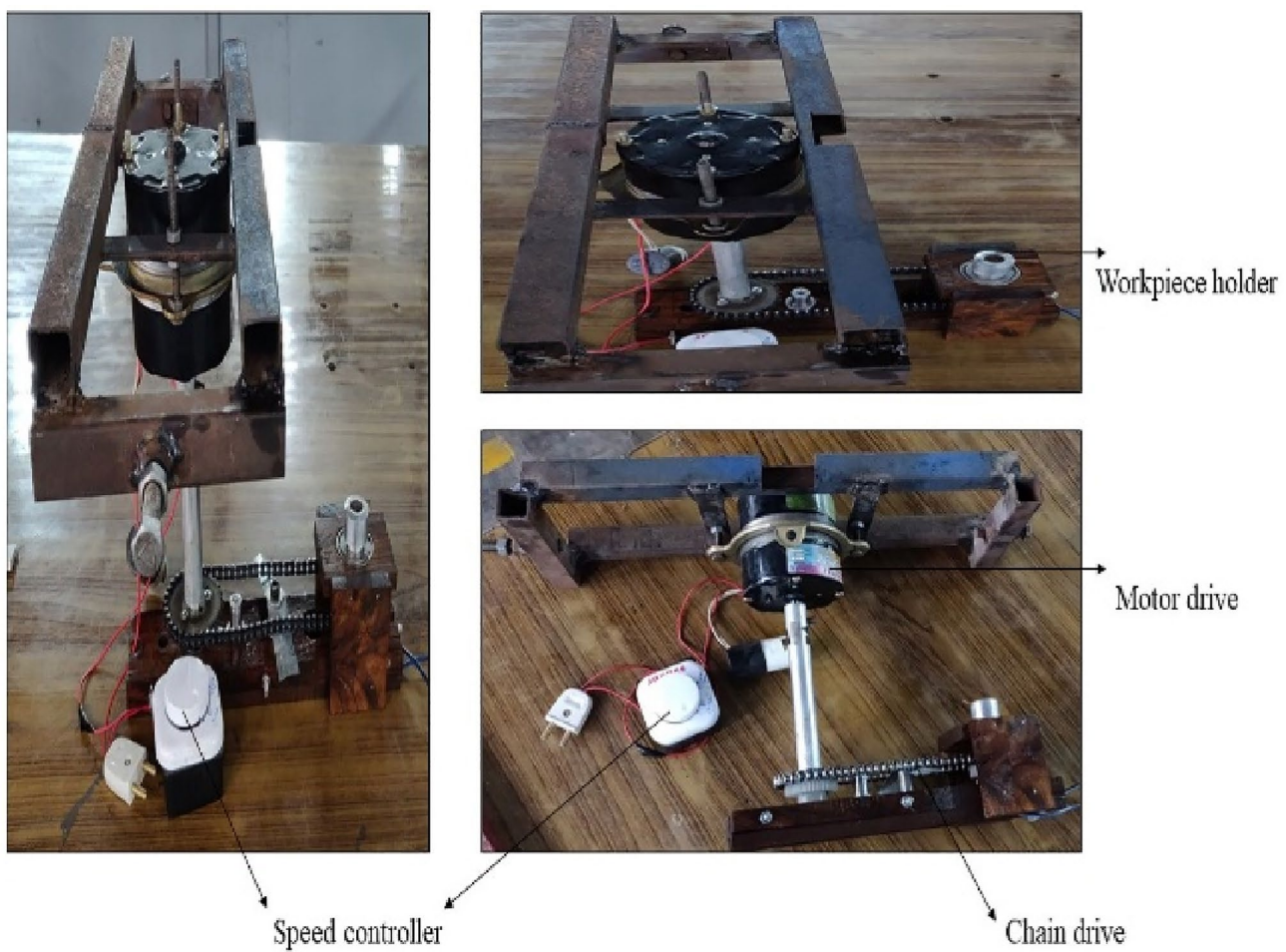


Fig. 6. Shows rotary workpiece setup used in RT-RW-EDM.

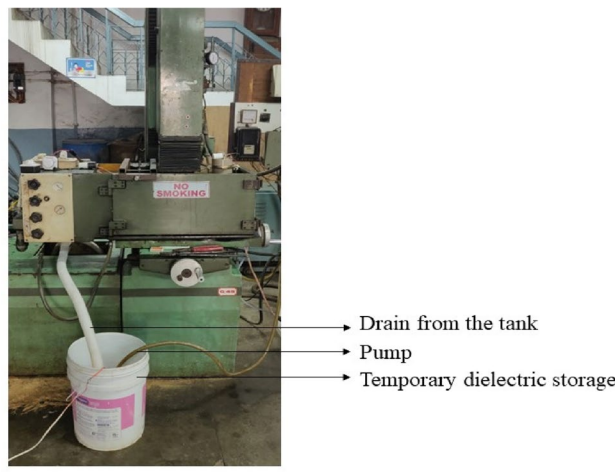


Fig. 7. Shows temporary arrangement made for bio-dielectrics.

Equipment's used

Design of experiment

Full factorial 127 orthogonal array was used for design of experiment. Process parameters selected were both electrodes rotation – as opposite direction rotation of both tool, same direction rotation of both tools and no rotation of both tools. Three dielectric – EDM oil, Biodiesel made from waste cooking oil (mustard oil) and distilled water with 10% ethanol mixed. Three tool – non treated Cu tool, heat-treated Cu tool and cryogenically

treated cu after heat-treated, Machining was done on at 311 μ s pulse on time and 6-amp pulse current⁶¹. The rotation of workpiece was kept as 900 rpm and rotation of tool was kept as 500 rpm⁴⁶. MRR, TWR and SR were measured as performance parameters.

The material removal rate was calculated using Eq. (1). The initial and final weight of workpiece were measured on digital weighing machine having a precision of 10^{-5} gm. A stopwatch was used for measuring machining time. The density of the composites was calculated using the Archimedes principle.

$$MRR = \frac{\text{initial weight} - \text{final weight}}{\text{Density} * \text{Machining time}} \quad (1)$$

The Tool wear rate was calculated using Eq. (2). The weight of tool before and after machining were measured on digital weighing machine and machining time was recorded on stop watch.

$$TWR = \frac{\text{initial weight} - \text{final weight}}{\text{Density} * \text{Machining time}} \quad (2)$$

The surface roughness was measured from portable Handy Surf (E-35A, Carl Zeiss) as shown in Fig. 8. Three copper tools were tested for microhardness-on-microhardness tester as shown in Fig. 9 and wear test on Pin on wear disc wear tester (Ducom, Model No: TR-201 CL, Bangalore, India) as shown in Fig. 10. Surface morphology images of machined samples⁶²⁻⁶⁴ were taken from JSM-6510LV make SEM machine in USIF lab AMU as shown in Fig. 11.

The results obtained were analysed through main effect, interaction plots, ANOVA and graphs. Predictive modelling in terms of regression analysis and multi objective optimization using grey relational analysis were also carried out.

Grey relational analysis

Grey relational analysis (GRA) provides an effective method for finding optimized solutions when dealing with conflicting responses. This approach offers the potential to validate multiple parameters while mitigating the shortcomings commonly associated with traditional statistical analyses⁶⁵. Hence GRA was used to optimize the experimental results as shown in Table 5. GRA has following steps.

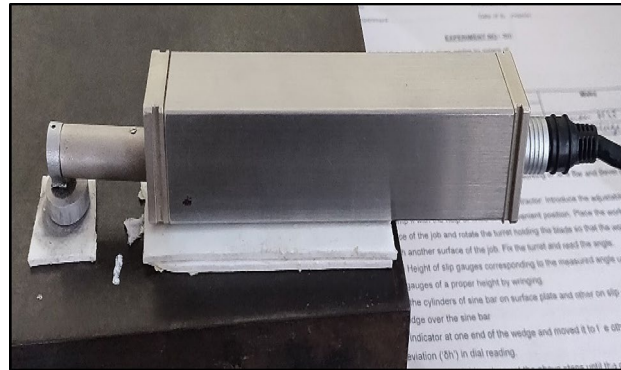


Fig. 8. Show Handy surf measuring surface roughness on the Al-10%SiC_{micro}-1%SiC_{nano} tablet.



Fig. 9. Shows the microhardness testing machine.



Fig. 10. Shows Pin on disc wear tester.



Fig. 11. Shows JSM-6510LV make SEM machine in USIF lab AMU.

1. Data is converted to signal to noise ratio which are then normalized between 0 and 1. Larger the better case Signal to noise ratio formulae is used for MRR as shown in Eq. (6) and smaller the better formulae is used for TWR and SR as shown in Eq. (4).

$$nij = -10\log\left(\frac{1}{n} \sum_{j=1}^n \frac{1}{yij^2}\right) \quad (3)$$

$$nij = -10\log\left(\frac{1}{n} \sum_{j=1}^n yij^2\right) \quad (4)$$

where n is the number of tests, Y_{ij} is the i th experiment at j th test.

The MRR reading are than normalized using the higher the better formula as shown in equation (5) and TWR, SR, Dilation in hole diameter and Hole taper are normalized using lower the better formula as shown in equation (6).

$$xi^*(k) = \frac{xi(k) - \min xi(k)}{\max xi(k) - \min xi(k)} \quad (5)$$

$$xi^*(k) = \frac{\max xi(k) - xi(k)}{\max xi(k) - \min xi(k)} \quad (6)$$

where $xi^*(k)$ is the value obtained after normalization, $\max xi$ is the largest value, $\min xi$ is the smallest value and $xi(k)$ is the target value from the experiment. These results are shown in Table 7.

2. Grey relational coefficient is calculated using formula shown in Eq. (7).

$$\xi_i[k] = \frac{\Delta_{\min} + \xi \Delta_{\max}}{\Delta_0 + \xi \Delta_{\max}} \quad (7)$$

where Δ_0 is the deviation sequence of the reference sequence $x_0^*(k)$ and the comparability sequence $x_i^*(k)$ as shown in equation (8).

$$\Delta o = ||x_0^*(k) - x_i^*(k)|| \quad (8)$$

$$\Delta_{\max} = \max \max ||x_0^*(k) - x_i^*(k)|| \quad (9)$$

$$\Delta_{\min} = \min \min ||x_0^*(k) - x_i^*(k)|| \quad (10)$$

ξ is distinguishing or identification coefficient: $\xi \in [0,1]$, ξ is generally taken as 0.5.

3. The average of the grey relational coefficient is calculated as the grey relational grade (yi) as shown in Eq. (11).

$$yi = 1/n \sum_{k=1}^n \xi_i[k] \quad (11)$$

Results

The machining of Al-10%SiC_{micro}-1%SiC_{nano} using different process parameters was performed as shown in Fig. 12. Three different dielectrics used are shown in Fig. 12. The machined samples are shown in Fig. 13. It is also visible that EDM oil and biodiesel left more carbon on the machined surface and distilled water with 10% ethanol provided much cleaner machined surface due to its lesser carbon content in same figure. The elemental compositions of samples are shown in Tables 3, 4 and Fig. 14. EDX results shows the presence of Al (68.77%) and Si (10.98%) in the surface of 23rd sample. These results confirm the content of the Al-10%SiC_{micro}-1%SiC_{nano} hybrid composites. The experimental results are displayed in Table 5.

Main effect plot

The main effect plot on the basis of mean and S/n ratio are shown in Figs. 15, 16, 17, 18, 19 and 20.



EDM oil with opposite tool and workpiece rotation.

Biodiesel with same direction rotation of tool and workpiece.

Distilled water-10% ethanol mixture with no tool and workpiece rotation.

Fig. 12. Shows EDM using different dielectrics as well as different rotation of tool and workpiece.

Opposite direction rotation of both electrodes

Same direction rotation of both electrodes

No rotation of both electrodes

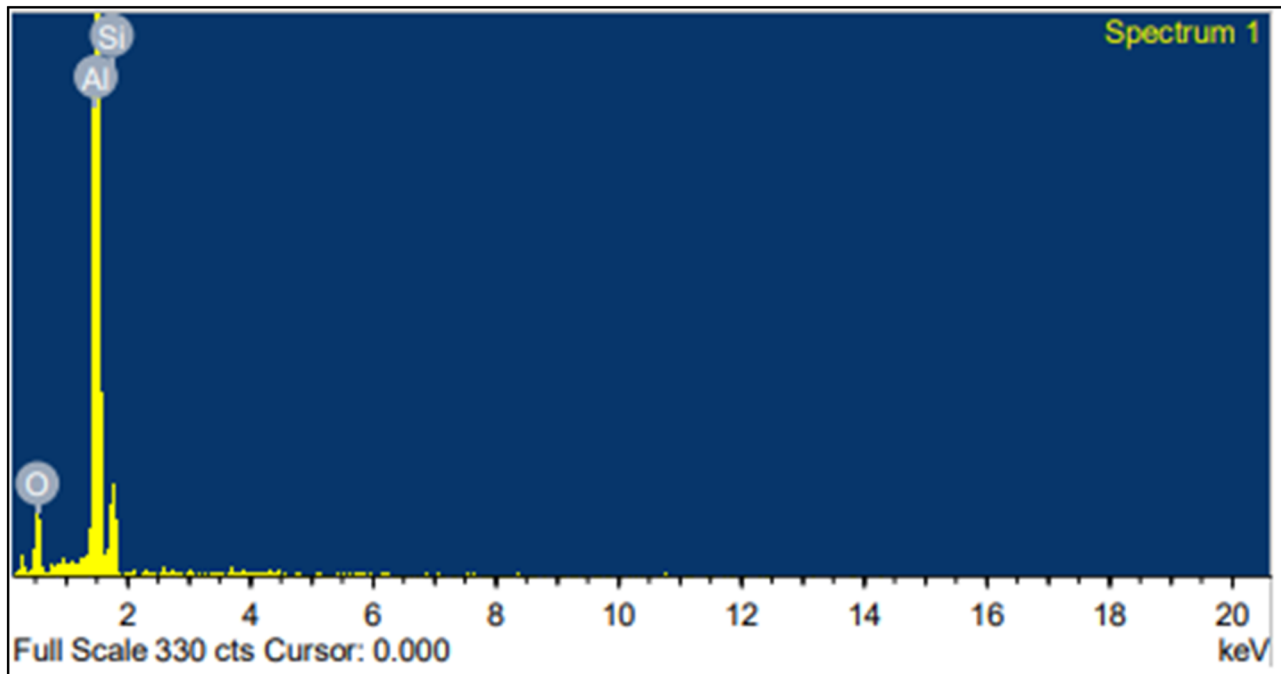


Fig. 13. Shows machined Al-10%SiC_{micro}-1%SiC_{nano} hybrid composite.

Copper tool	Microhardness	Porosity	Wear rate/min
Non treated tool	395 HV	0.000844	0.000689
Heat treated tool	366 HV	0.000845	0.001457
Cryogenic treated tool	343 HV	0.001017	0.001121

Table 3. Shows different properties of Copper Tool.

Element	Weight %	Atomic %
O	20.25	30.10
Al	68.77	60.60
Si	10.98	9.30

Table 4. Shows the elemental composition of 23 workpiece sample.**Fig. 14.** Shows the EDX test performed on 23 sample.

ANOVA

Interaction plot

The interaction plots are shown in Figs. 21, 22 and 23.

Scanning electron microscope

Scanning electron microscope (SEM) images of machining using distilled water having 10% ethanol are shown in Fig. 24. SEM images of machining using EDM oil dielectric are shown Fig. 25. SEM images of machining using biodiesel dielectric are shown in Fig. 26. Small craters are visible in all SEM images due to evacuation of SiC particles. Since reinforcement particles such as SiC have high melting temperature which is not attainable in EDM. As result these particles evacuate their places once the melting temperature of matrix material (Al) is reached, leaving behind small craters. Also, lot of resolidified globules of matrix are visible in most SEM images. Size of globules seems to be larger when composite is machined using biodiesel followed by EDM oil and Biofuel. SEM image of the tools is shown in Figs. 27, 28 and 29.

Empirical model

The current work involved the development of empirical models using general regression analysis for all performance characteristics, based on the experimental results obtained. This approach has been employed by many

S.no	Tool and workpiece rotation	Tool treatment	Dielectric	Time taken	Initial weight	Final weight	Density of MCC	MRR	Initial tool weight	Final tool weight	TWR	SR
1	Opposite direction	HTT	Water-ethanol	2.383	1.484	1.3588	1.680634	31.25693175	19.125	19.1163	0.407405	2.375
2	Opposite direction	NTT	EDM oil	1.000	1.389	1.353	1.675513	21.48596112	28.9169	28.9156	0.145089	2.5
3	No rotation	CTT	Water-ethanol	2.767	1.393	1.3501	1.75662	8.827191033	27.325	27.3145	0.423569	2.175
4	Same direction	CTT	Water-ethanol	2.683	1.42	1.32	1.742331	21.38920479	27.3082	27.2989	0.386812	2.375
5	No rotation	HTT	Water-ethanol	2.583	1.389	1.3832	1.700122	1.32058803	19.1269	19.1237	0.138249	2.825
6	Same direction	HTT	Water-ethanol	2.367	1.345	1.2536	1.857735	20.78860673	19.1152	19.1076	0.3584	2.4
7	Same direction	HTT	EDM oil	1.050	1.434	1.4081	1.703088	14.48349605	19.1437	19.14	0.393282	2.325
8	No rotation	NTT	EDM oil	2.183	1.438	1.323	1.73253	30.40163926	28.9166	28.9155	0.05623	2.75
9	Opposite direction	HTT	EDM oil	2.367	1.406	1.2855	1.712546	29.73088173	19.1475	19.1441	0.160337	1.725
10	No rotation	HTT	Bio diesel	2.483	1.406	1.3383	1.714634	15.89945297	19.1338	19.13	0.170781	3.325
11	Same direction	NTT	Water-ethanol	2.483	1.398	1.3119	1.728059	20.06362877	28.8941	28.8832	0.489873	2.5
12	Same direction	NTT	EDM oil	1.333	1.435	1.4274	1.690224	3.372334495	28.9183	28.92	-0.1423	2.4
13	Opposite direction	CTT	Bio diesel	2.367	1.41	1.346	1.702899	15.88013185	27.3274	27.326	0.066021	2.35
14	Opposite direction	CTT	EDM oil	2.667	1.42	1.3225	1.686461	21.68001761	27.3433	27.3397	0.15067	2.275
15	Same direction	NTT	Bio diesel	2.533	1.386	1.2697	1.709001	26.86241171	28.9104	28.908	0.105733	2.4
16	No rotation	NTT	Water-ethanol	2.200	1.414	1.406	1.665489	2.183361193	28.9062	28.8996	0.334821	2.725
17	No rotation	HTT	EDM oil	1.417	1.391	1.281	1.719407	45.15921681	19.1443	19.1425	0.141807	2.125
18	No rotation	CTT	EDM oil	1.283	1.415	1.3083	1.723508	48.2404846	27.3392	27.338	0.10436	2.3
19	Same direction	CTT	EDM oil	1.750	1.397	1.3379	1.659145	20.3547193	27.3379	27.337	0.057398	2.2
20	Same direction	HTT	Bio diesel	2.150	1.4249	1.3408	1.700561	23.00198627	19.1325	19.1301	0.124585	3.05
21	No rotation	NTT	Bio diesel	2.317	1.4	1.3408	1.719902	14.85780062	28.9096	28.908	0.077081	3.6
22	Opposite direction	CTT	Water-ethanol	2.333	1.419	1.3592	1.796203	14.26819692	27.3189	27.3085	0.497449	3.025
23	Opposite direction	NTT	Water-ethanol	2.333	1.379	1.2799	1.770218	23.99219932	28.9059	28.8949	0.526148	2.55
24	Opposite direction	NTT	Bio diesel	2.517	1.415	1.2679	1.738329	33.62443077	28.9077	28.9074	0.013304	2.525
25	Opposite direction	HTT	Bio diesel	2.333	1.386	1.2994	1.758883	21.10105133	19.1301	19.1279	0.10523	4.175
26	No rotation	CTT	Bio diesel	2.367	1.44	1.3803	1.714286	14.71478873	27.3299	27.3279	0.094316	4.075
27	Same direction	CTT	Bio diesel	2.333	1.459	1.3894	1.72255	17.31651816	27.33	27.3279	0.100446	3.7

Table 5. Showing experimental results.

researchers previously^{66–68}. The model's performance was evaluated using MRR, TWR, and SR, with R^2 values of 96.87%, 94.79%, and 90.27%, respectively. To assess the effectiveness of the proposed multivariate approach, a residual analysis was conducted to verify the model's adequacy. The data was found to be normally distributed, and the homogeneity of MRR data was confirmed in the fitted plot. The normal probability plot of the standardized residual, standardized residual versus observation order, fitted value, and histogram are shown in Figs. 30, 31 and 32. These figures indicate that there are no outliers, and the process follows a normal distribution. The straight-line pattern of the residual points in the normal probability plot suggests that the proposed model fits the data well. Furthermore, the standardized residuals and observation orders do not exhibit any pattern or structure, as evident from Figs. 30, 31 and 32. Overall, it can be concluded that the recommended model performs satisfactorily.

The regression equations are shown in Eqs. (12), (13) and (14) where Opposite direction rotation of both electrodes is denoted as R_o , Same direction rotation of both electrodes is denoted as R_s , no rotation of both electrodes is denoted as R_n , Distilled Water- 10% ethanol is denoted as DE, Biodiesel is denoted as BD, EDM oil is denoted as EO.

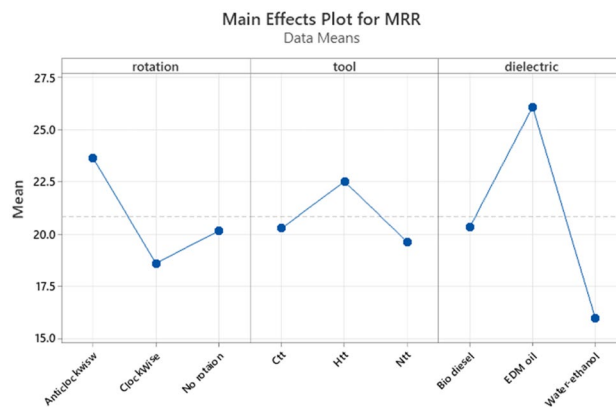


Fig. 15. Shows main effect plot for MRR (mean).



Signal-to-noise: Larger is better

Fig. 16. Shows main effect plot for MRR (S/N ratio).

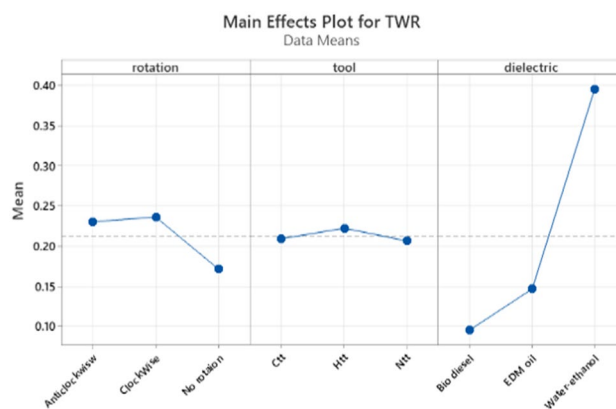


Fig. 17. Shows main effect plot for TWR (mean).

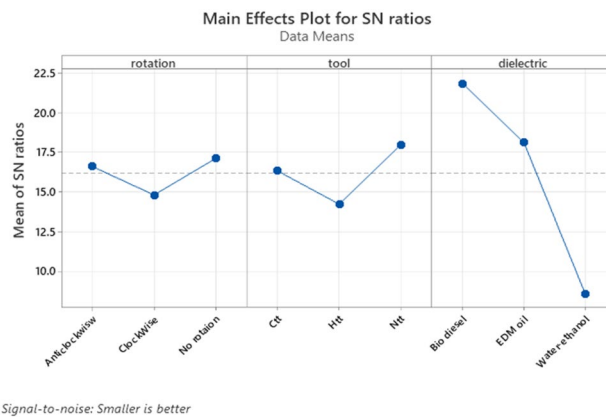


Fig. 18. Shows main effect plot of TWR (S/N ratio).

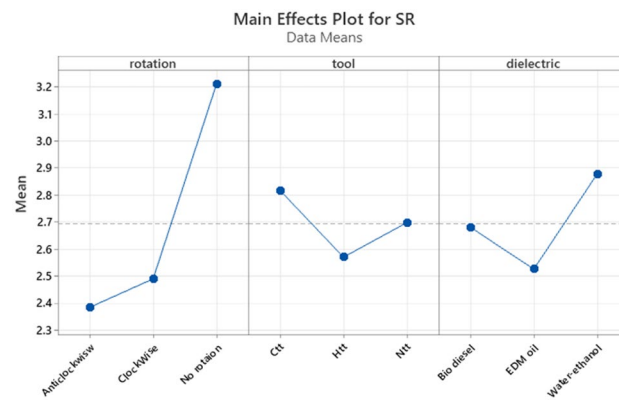


Fig. 19. Shows main effect plot for SR (mean).

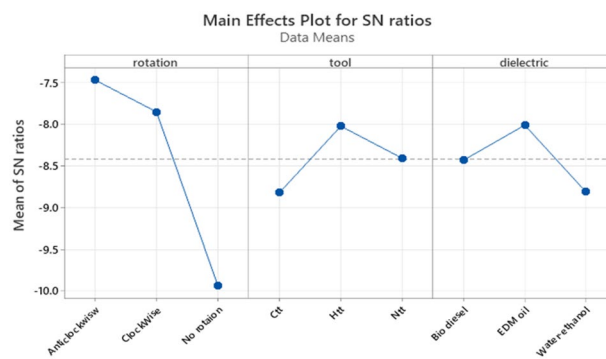


Fig. 20. Shows main effect plot for SR (S/N ratio).

Interaction Plot for MRR

Data Means

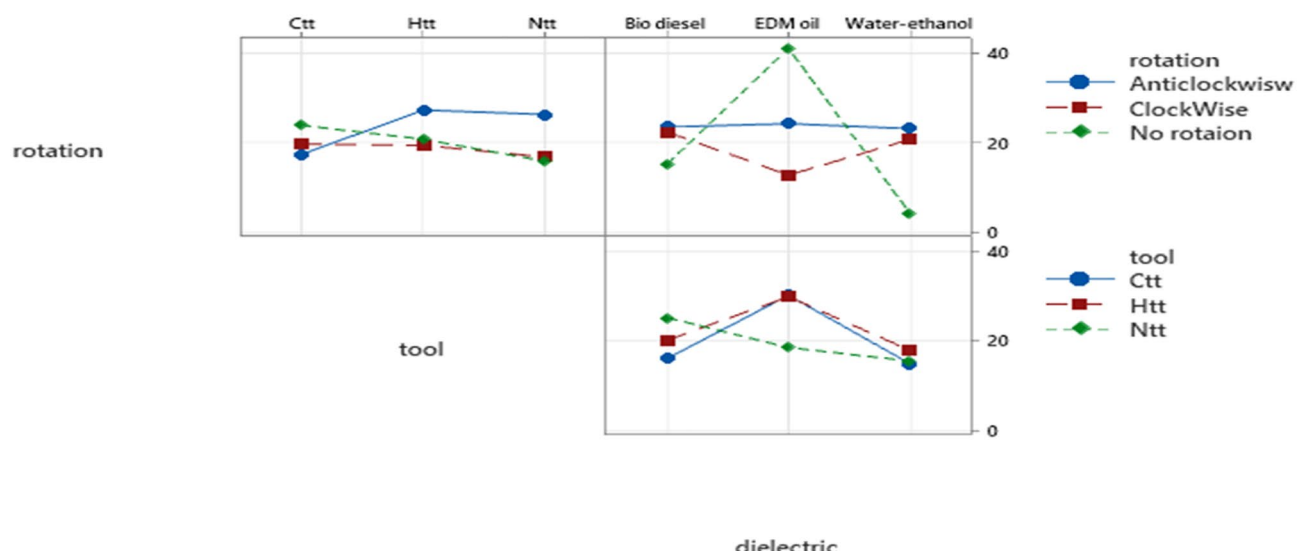


Fig. 21. Shows interaction plot for MRR.

Interaction Plot for TWR

Data Means

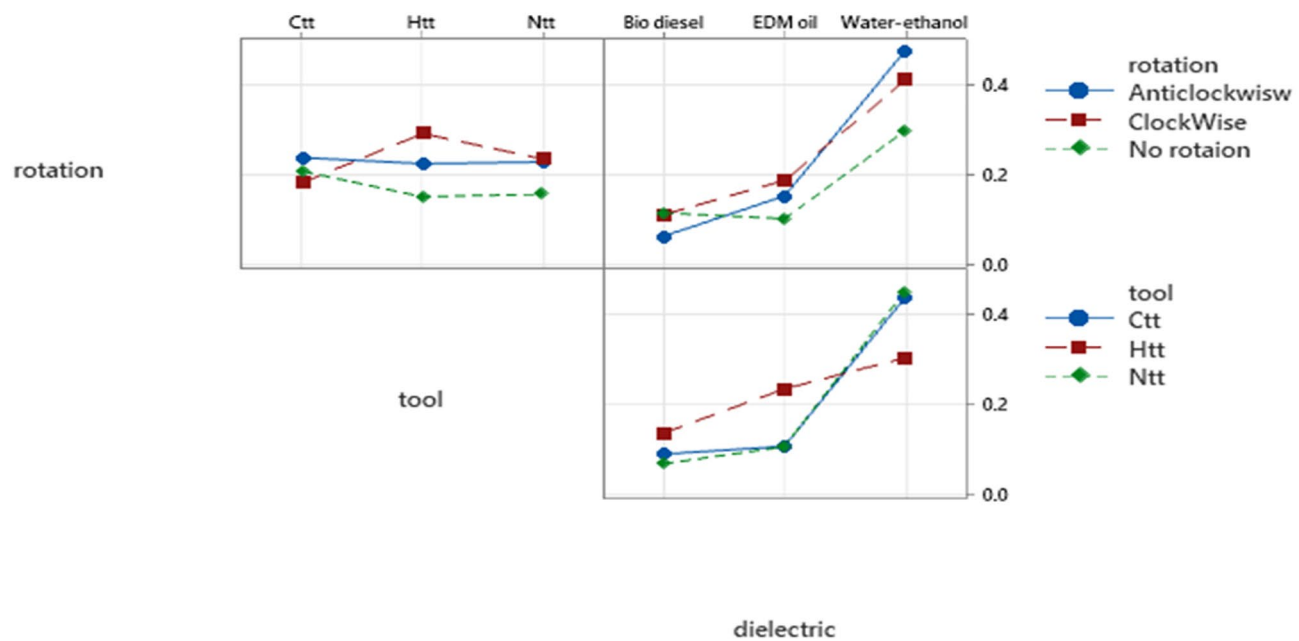


Fig. 22. Shows the interaction plot for TWR.

Interaction Plot for SR Data Means

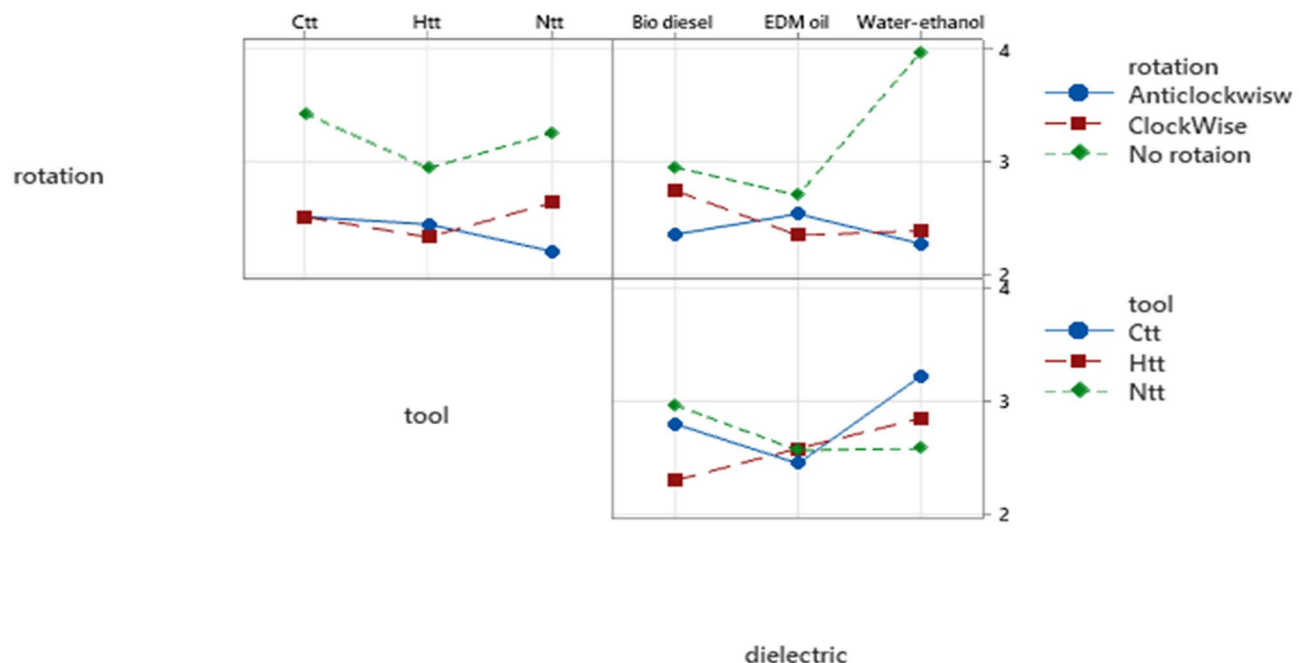


Fig. 23. Shows interaction plot for SR.

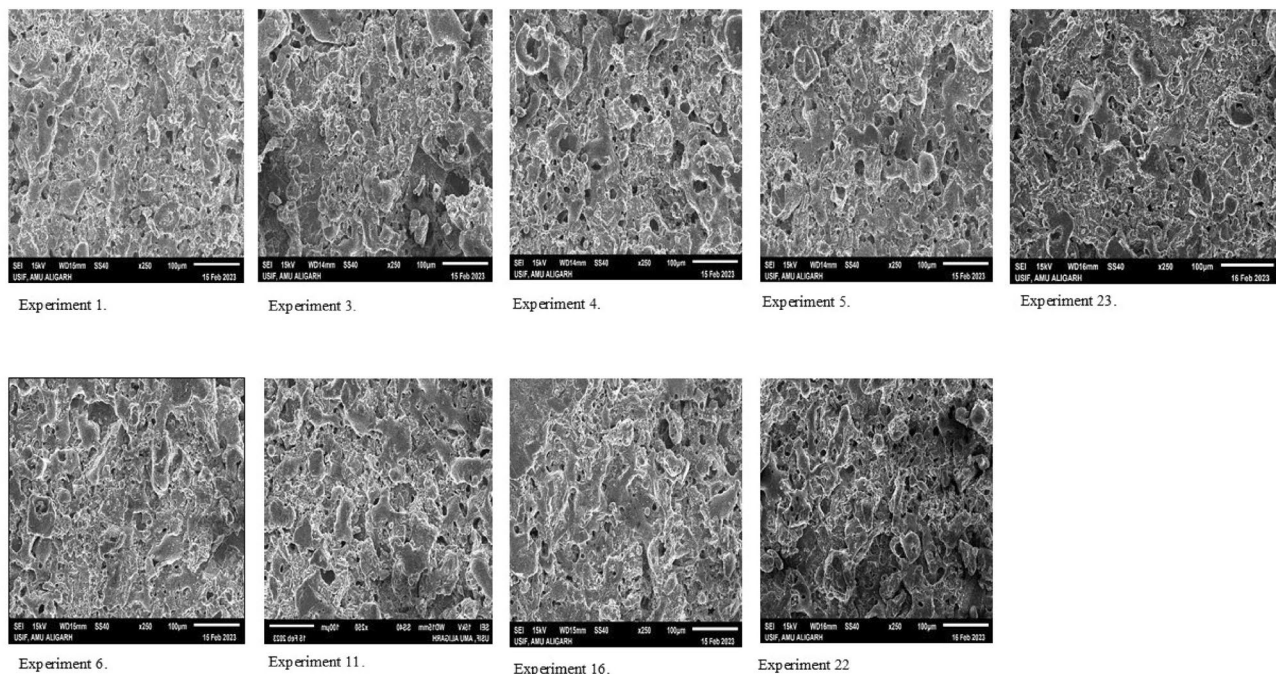
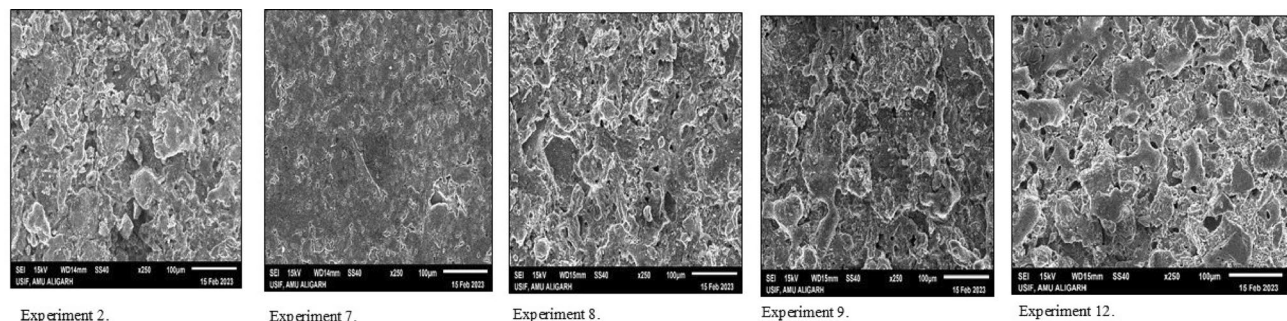


Fig. 24. SEM image of Al-10%SiC_{micro}-1%SiC_{nano} hybrid composite machined using Bio fuel as Dielectric.



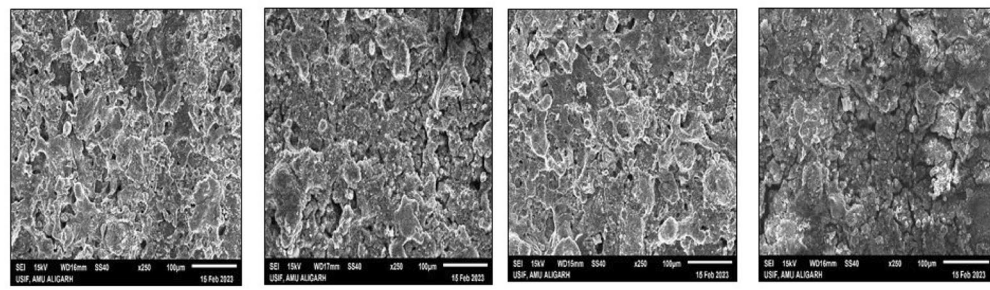
Experiment 2.

Experiment 7.

Experiment 8.

Experiment 9.

Experiment 12.



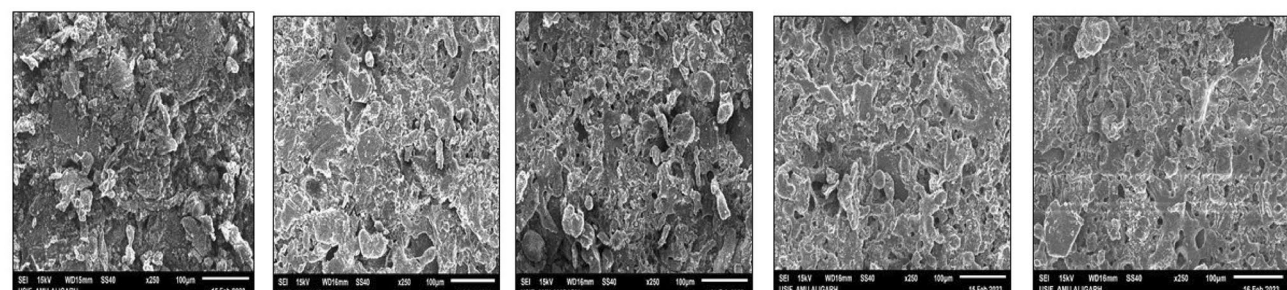
Experiment 14.

Experiment 17.

Experiment 18.

Experiment 19

Fig. 25. SEM image of Al-10%SiC_{micro}-1%SiC_{nano} hybrid composite machined using EDM oil as Dielectric.



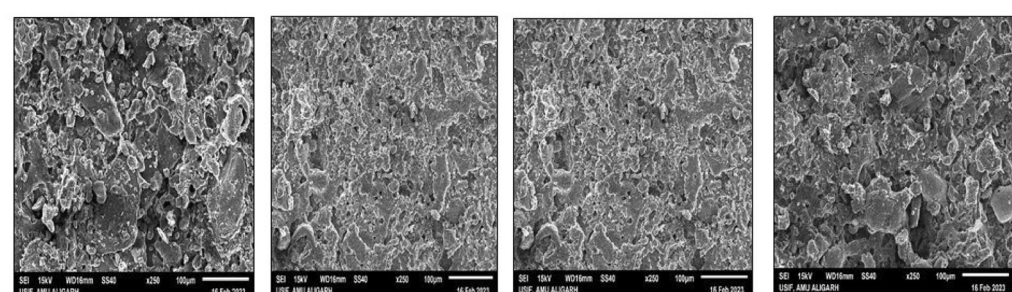
Experiment 10.

Experiment 13

Experiment 15.

Experiment 20.

Experiment 21.



Experiment 24.

Experiment 25.

Experiment 26.

Experiment 27

Fig. 26. SEM image of Al-10%SiC_{micro}-1%SiC_{nano} hybrid composite machined using Biodiesel as Dielectric.

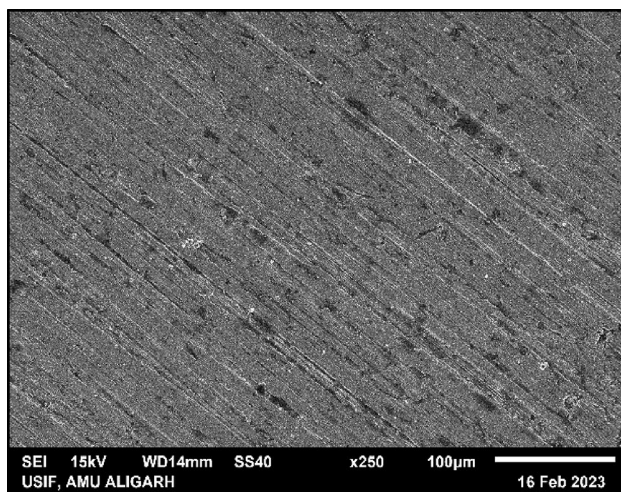


Fig. 27. Shows SEM image of cryogenic treated tool.

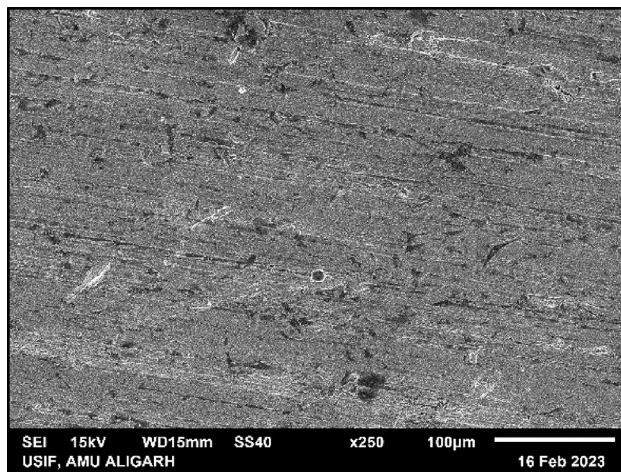


Fig. 28. Shows SEM image of heat-treated tool.

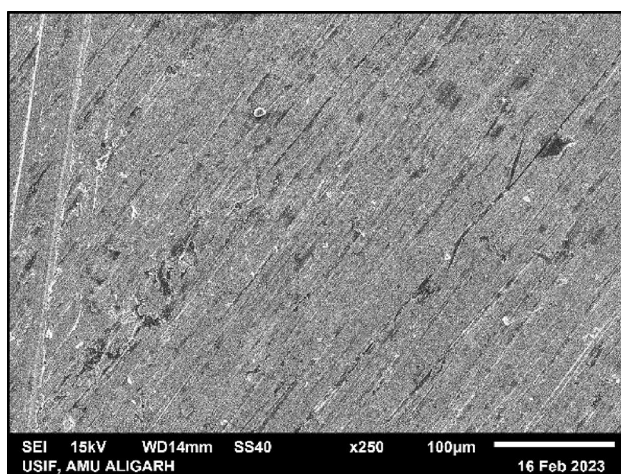


Fig. 29. Shows SEM image of non-treated tool.

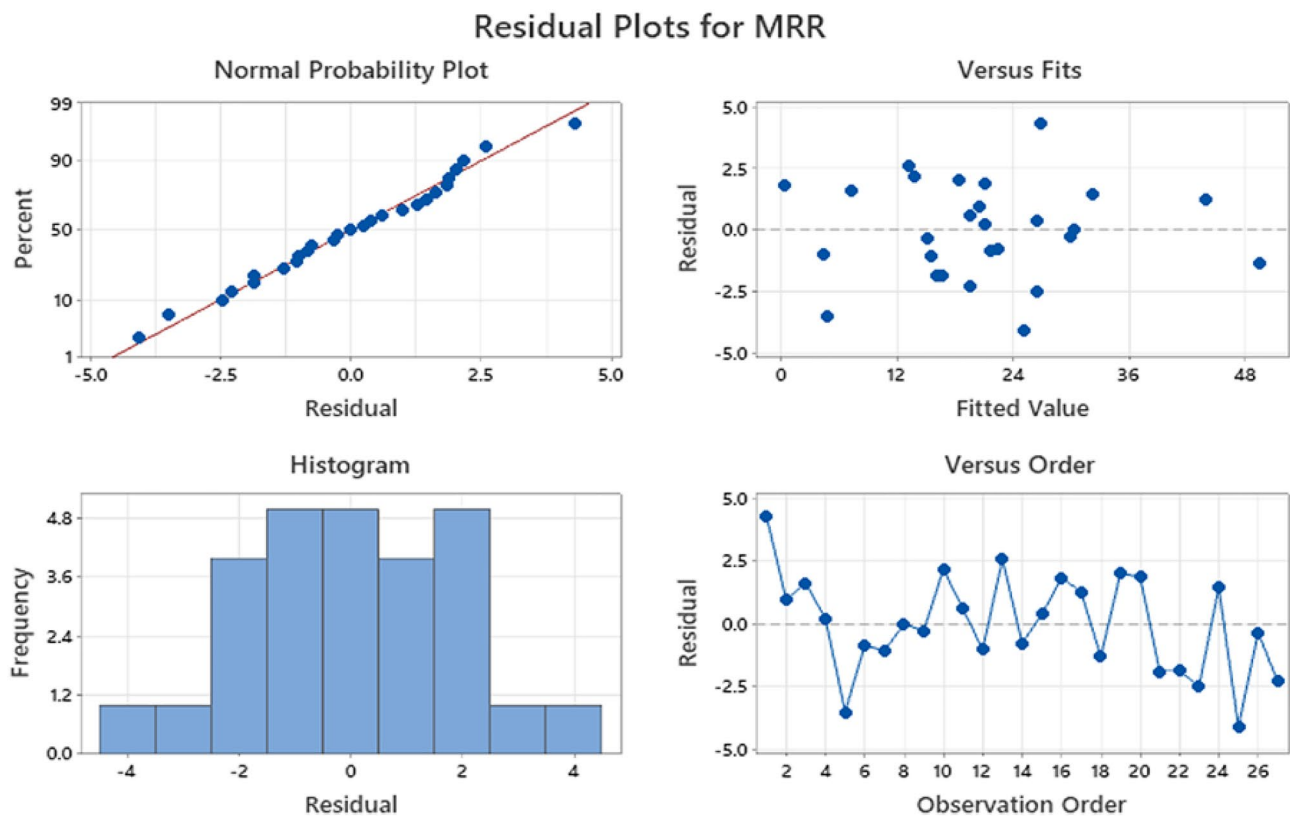


Fig. 30. Shows residual plots for MRR.

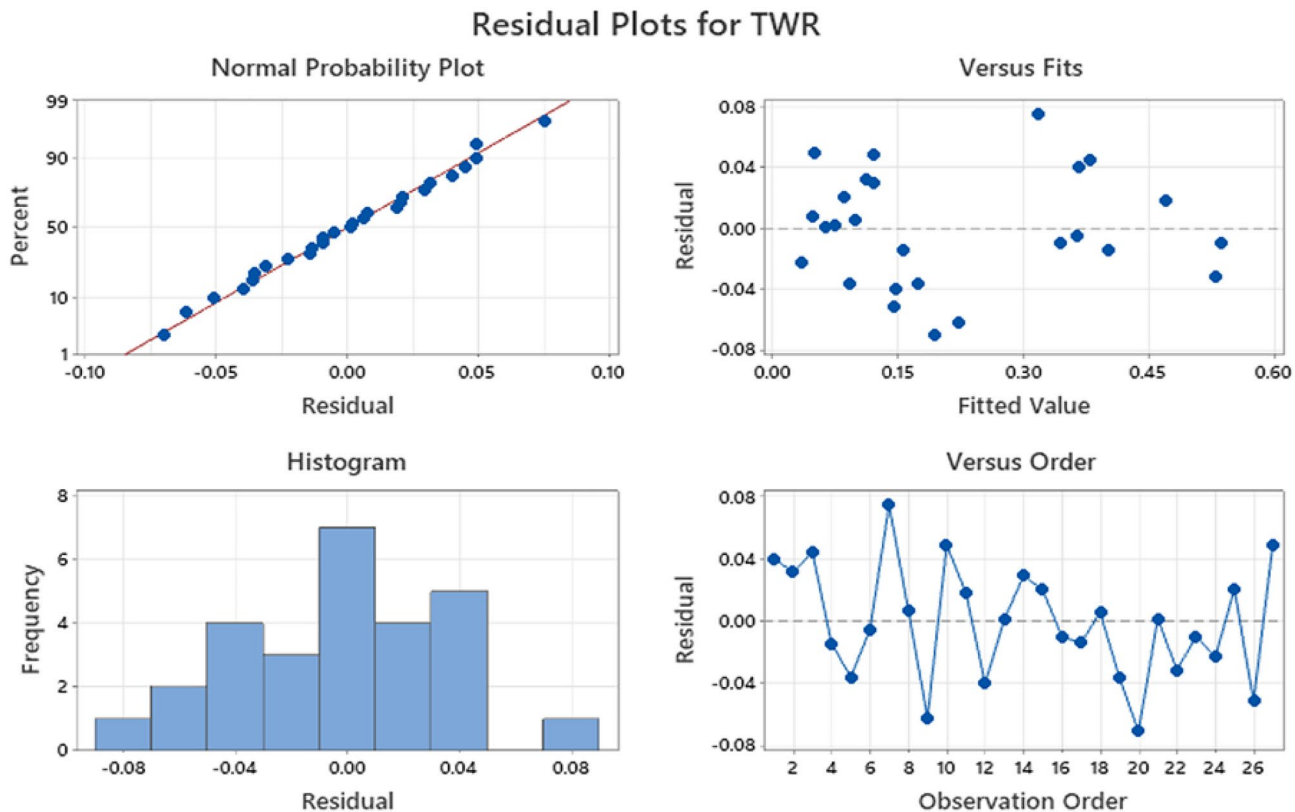


Fig. 31. Shows residual plots for TWR.

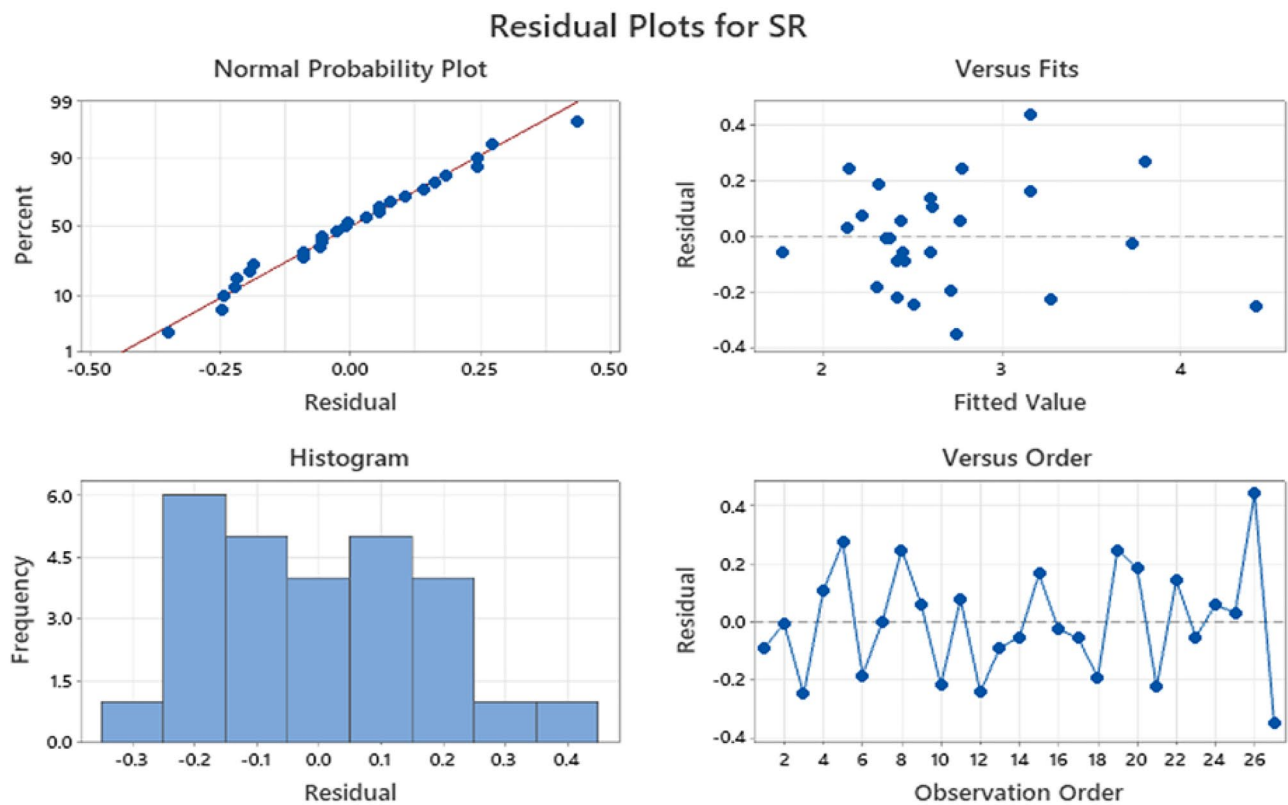


Fig. 32. Shows residual plots for SR.

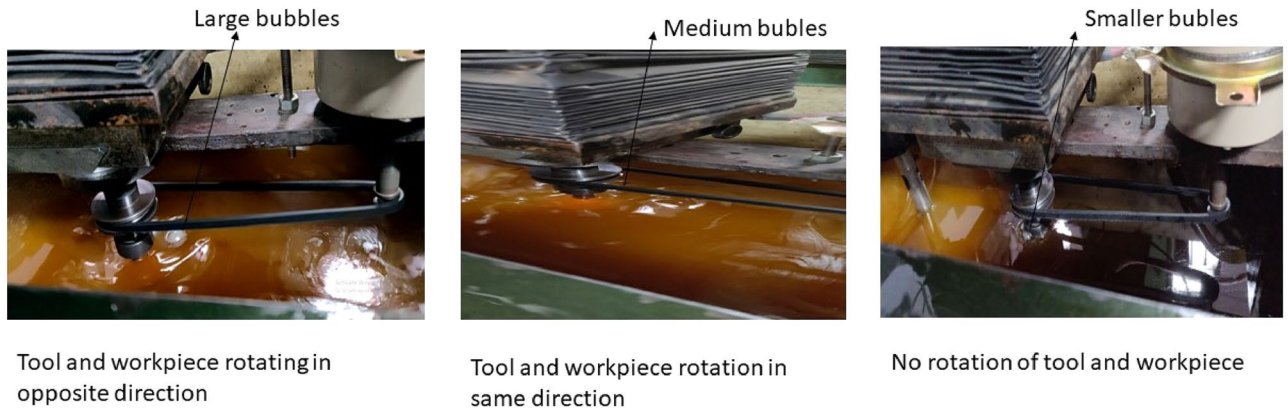
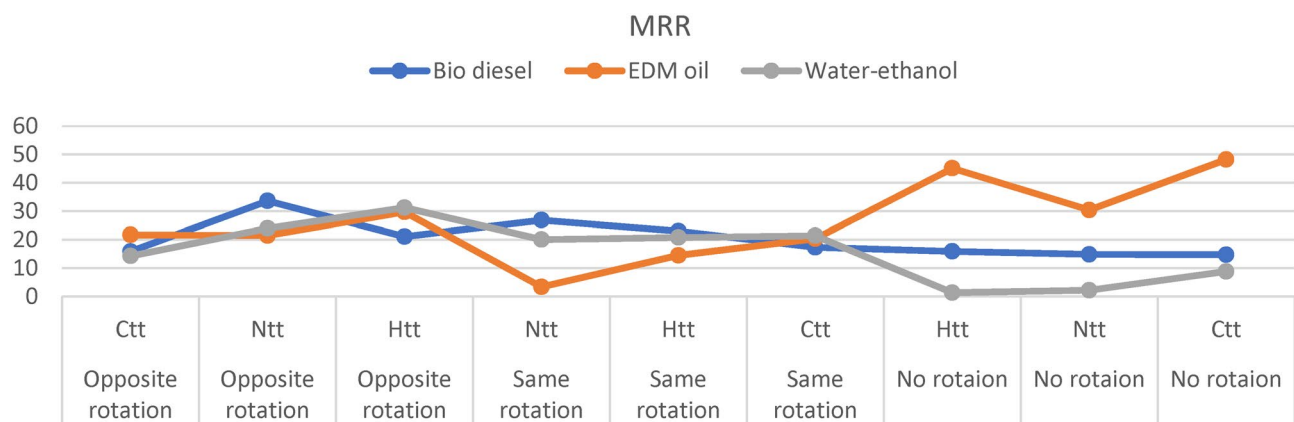


Fig. 33. Shows bubbles during EDM.

$$\begin{aligned}
 MRR = & 20.824 + 2.845 R_o - 2.198 R_s - 0.646 R_n - 0.528 CTT + 1.703 HTT - 1.175 NTT - 0.462 BD + 5.277 EO - 4.814 DE - 5.87 R_o * CTT + \\
 & 1.99 R_o * HTT + 3.87 R_o * NTT + 1.59 R_s * CTT - 0.90 R_s * HTT - 0.68 R_s * NTT + 4.28 R_n * CTT - 1.09 R_n * HTT - 3.19 R_n * NTT + 0.33 R_o * BD - \\
 & 4.65 R_o * EO + 4.32 R_o * WE + 4.23 R_s * BD - 11.17 R_s * EO + 6.94 R_s * WE - 4.56 R_n * BD + 15.81 R_n * EO - 11.25 R_n * WE - 3.86 CTT * BD + 4.52 \\
 & CTT * EO - 0.65 CTT * WE - 2.06 HTT * BD + 1.99 HTT * EO + 0.08 Htt * WE + 5.93 NTT * BD - 6.51 NTT * EO + 0.58 NTT * WE. \tag{12}
 \end{aligned}$$

Source	DF	Adj SS	Adj MS	F-Value	P-Value	Percentage contribution
MRR						
Both electrodes rotation	2	120.08	60.04	4.74	0.044	3.71
Tool treatment	2	41.02	20.51	1.62	0.256	1.26
Dielectric	2	461.11	230.56	18.22	0.001	14.25
Both electrodes rotation* Tool treatment	4	260.47	65.12	5.15	0.024	8.05
Both electrodes rotation*Dielectric	4	1885.38	471.35	37.25	0.000	58.28
Tool treatment*Dielectric	4	365.37	91.34	7.22	0.009	11.29
Error	8	101.24	12.65			3.12
Total	26	3234.67				100
TWR						
Both electrodes rotation	2	0.023	0.011	2.66	0.130	3.46
Tool treatment	2	0.001	0.0006	0.15	0.863	0.19
Dielectric	2	0.465	0.232	53.42	0.000	69.55
Both electrodes rotation* Tool treatment	4	0.023	0.005	1.34	0.336	3.47
Both electrodes rotation *Dielectric	4	0.041	0.010	2.40	0.136	6.25
Tool treatment *Dielectric	4	0.079	0.019	4.55	0.033	11.84
Error	8	0.034	0.004			5.20
Total	26	0.669				100
SR						
Both electrodes rotation	2	3.65	1.82	15.75	0.002	38.30
Tool treatment	2	0.27	0.13	1.19	0.354	2.88
Dielectric	2	0.56	0.28	2.43	0.150	5.89
Both electrodes rotation* Tool treatment	4	0.39	0.09	0.86	0.526	4.19
Both electrodes rotation *Dielectric	4	2.61	0.65	5.64	0.019	27.43
Tool treatment *Dielectric	4	1.10	0.27	2.38	0.138	11.55
Error	8	0.92	0.11			9.72
Total	26	9.53				100

Table 6. Shows ANOVA results.**Fig. 34.** Shows the MRR obtained from each dielectric.

$$\begin{aligned}
 \text{TWR} = & 0.2125 + 0.0177 R_o + 0.0236 R_s - 0.0413 R_n - 0.0035 \text{ CTT} + 0.0097 \text{ HTT} - 0.0062 \text{ NTT} \\
 & - 0.1172 \text{ BD} - 0.0661 \text{ EO} + 0.1833 \text{ WE} + 0.0114 R_o * \text{ CTT} - 0.0156 R_o * \text{ HTT} \\
 & + 0.0042 R_o * t - 0.0511 R_s * \text{ CTT} + 0.0462 R_s * \text{ HTT} + 0.0048 R_s * \text{ NTT} + 0.0397 R_n * \text{ CTT} \\
 & - 0.0307 R_n * \text{ HTT} - 0.0090 R_n * \text{ NTT} - 0.0514 R_o * \text{ BD} \\
 & - 0.0121 R_o * \text{ EO} + 0.0635 R_o * \text{ WE} - 0.0086 R_s * \text{ BD} \\
 & + 0.0164 R_s * \text{ EO} - 0.0078 R_s * \text{ WE} + 0.0601 R_n * \text{ BD} - 0.0044 R_n * \text{ EO} - 0.0557 R_n * \text{ WE} - 0.0048 \text{ CTT} * \text{ BD} \\
 & - 0.0388 \text{ CTT} * \text{ EO} + 0.0436 \text{ CTT} * \text{ WE} + 0.0286 \text{ HTT} * \text{ BD} + 0.0757 \text{ HTT} * \text{ EO} - 0.1042 \text{ HTT} * \text{ WE} \\
 & - 0.0237 \text{ NTT} * \text{ BD} - 0.0369 \text{ NTT} * \text{ EO} + 0.0606 \text{ NTT} * \text{ WE}.
 \end{aligned} \tag{13}$$

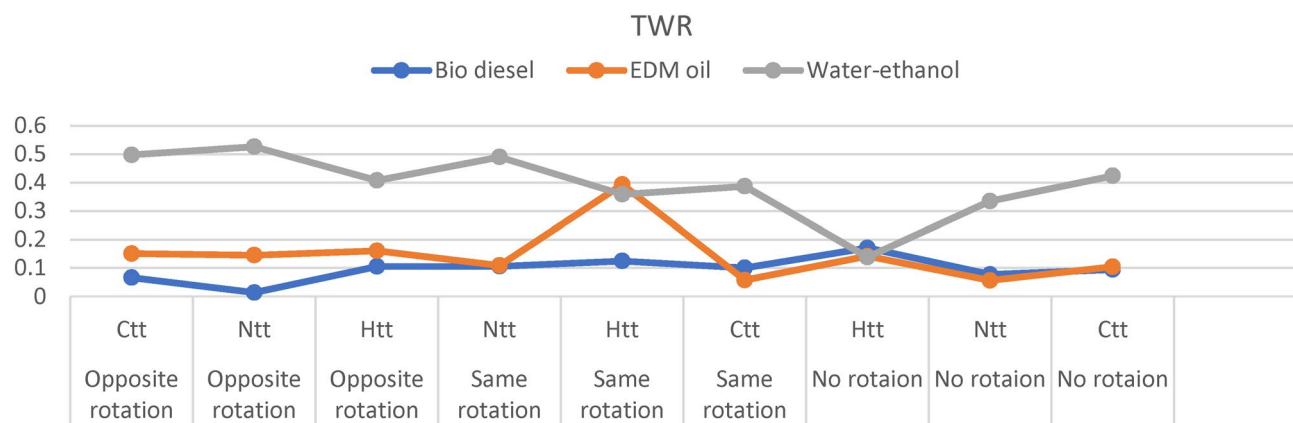


Fig. 35. Shows TWR obtained for each experiment.

$$\begin{aligned}
 SR = & 2.6944 - 0.3111R_o - 0.2056R_s + 0.5167R_n + 0.1222 CTT - 0.1250 HTT + 0.0028 NTT - 0.0139 BD - 0.1694 EO + 0.1833 WE + 0.003 \\
 R_o * CTT + & 0.183R_o * HTT - 0.186R_o * NTT - 0.103R_s * CTT - 0.039R_s * HTT + 0.142R_s * NTT + 0.100 R_n * CTT - 0.144 R_n * HTT + 0.044 \\
 R_n * NTT - & 0.019R_o * BD + 0.319R_o * EO - 0.300R_o * WE + 0.267R_s * BD + 0.022R_s * EO - 0.289 R_s * WE - 0.247 R_n * BD - 0.342 R_n * EO + 0.589 \quad (14) \\
 R_n * WE - & 0.011 CTT * BD - 0.206 CTT * EO + 0.217 CTT * WE - 0.264 HTT * BD + 0.175 HTT * EO \\
 + & 0.089 HTT * WE + 0.275 NTT * BD + 0.031 NTT * EO - 0.306 NTT * WE.
 \end{aligned}$$

Discussion

In order to improve sustainability in the EDM process, this study utilized biodiesel and Bio-fuel (a mixture of distilled water and 10% ethanol) as bio dielectrics. Additionally, the study explored the impact of process parameters, such as the direction of rotation for both electrodes (same direction, opposite direction, or no rotation), on the performance parameters of EDM. Further, three types of copper tools were used, including a non-treated copper tool, a heat-treated (annealed) copper tool, and a cryogenically treated copper tool. The novelty of this work lies in the use of both electrode rotation, the use of bio-fuel (distilled water mixed with 10% ethanol) as a bio dielectric, and the use of heat-treated copper tools. The workpiece used in this study was Al-10%SiC_{micro}-1%SiC_{nano}, which was prepared using powder metallurgy processes.

Efficient flushing is critical for effective machining, and it is well-known that the frequency of bubbles formed during the process is a key factor in achieving this Ref.¹⁴. The size of the bubbles depends on the viscosity of the dielectric being used, with biodiesel having the highest viscosity and a distilled water and ethanol mixture having the lowest. Consequently, larger bubbles were observed in biodiesel, while the smallest bubbles were formed in distilled water with 10% ethanol mixture. The purplish colour of the flames observed in the latter case was due to the reducing nature of ethanol as seen in Fig. 12. When the tool and workpiece were rotated in opposite directions, the highest number of bubbles were observed, which were also larger in size. Conversely, no rotation resulted in smaller bubbles, and resultantly more material deposition was observed on the tool. When the tool and workpiece were rotated in the same direction, medium-sized bubbles were observed as shown in Fig. 33.

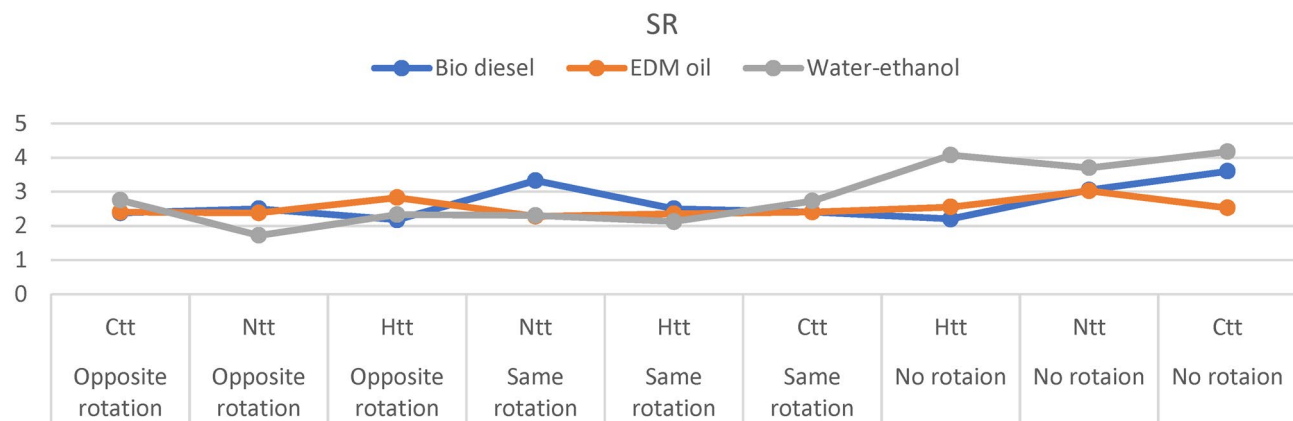


Fig. 36. Shows SR obtained for each experiment.

Bio-dielectrics

According to ANOVA Table 6, Dielectrics contributed 14% to the MRR and had a significant impact on it ($p < 0.05$). From the main effect plot of MRR (Figs. 15, 17), it was observed that the EDM oil provided the highest MRR followed by Biodiesel and Distilled water mixed with 10% ethanol. However, literature indicates that biodiesel typically yields more MRR than conventional oil^{23,60}. This is because the high viscosity of biodiesel hampers the expansion of the generated bubbles created in the discharging zone, resulting in higher pressure over the discharge zone, which increases the impulsive force acting on the machined surface due to the contraction and expansion of the discharge-generated bubbles. Therefore, biodiesel provides higher energy density and more efficient energy transfer between electrodes, leading to higher MRR. The same can be seen in Fig. 33.

By analysing each reading of MRR in Fig. 34, it was found that for most experiments, biodiesel and Distilled water mixed with 10% ethanol provided better readings than EDM oil, except in the case of no rotation. For the no rotation case, the use of the built-in flushing system/pump provided much better flushing/debris removal, leading to more visible MRR for EDM oil. However, the secondary/makeshift flushing arrangements made for biodiesel could not provide the same flushing rate, partially due to the high viscosity of the biodiesel being used, resulting in inefficient flushing and a lower MRR. For the case of distilled water mixed with 10% ethanol, least viscosity and lower probability of oxidation should also lead to improved machining efficiency. However, in this case, MRR readings were reduced for the no rotation case due to machining error, resulting in a lack of visible sparks during machining. Overall, on average, EDM oil provided the most MRR (Fig. 15), but for 6 out of 9 experiments, both bio-dielectrics outperformed EDM oil in terms of MRR.

From ANOVA Table 6 it was observed that Dielectric contributed 69% to TWR Dielectrics also significantly affected TWR ($p < 0.05$). Valaki et al.³³ also achieved similar results. From main effect plot of TWR Fig. 17 it was observed that EDM oil gave second most TWR. Biodiesel gave least TWR as Biodiesel made from waste vegetable oil (mustard oil) has higher flash point, more viscosity and better lubricating properties than EDM oil which results in reduced arcing, hence reduced TWR³³. Distilled water mixed with 10% ethanol gave most TWR. From Fig. 35 same thing is observed for most of the experiments.

The ANOVA Table 6 revealed that Dielectric contributed 5.89% to SR. Based on the main effect plot of SR depicted in Fig. 20, it was evident that the EDM oil had the least SR. The second larger SR was observed for biodiesel, which could be attributed to its higher viscosity that caused greater resistance in the expansion of bubbles generated during the process. This led to higher pressure and impulse force acting on the surface, resulting in a rougher surface texture. On the other hand, the use of distilled water mixed with 10% ethanol as a dielectric resulted in the highest SR.

From Fig. 36 it was observed that biodiesel and EDM oil gave similar SR reading for most experiment but Distilled water mixed with 10% ethanol gave least SR for 6 out of 9 experiments. However, in case of no rotation experiments, the SR obtained from Distilled water with 10% ethanol was high which can be attributed to abnormal sparking observed due to some machining error. Besides the use of Distilled water with 10% ethanol dielectric produced much cleaner machined surfaces as shown in Fig. 13. Since distilled water with 10% ethanol has only 5.71% carbon which was much less than other two dielectrics. At high temperatures the carbon debris creation is much less due decomposition of hydrocarbon-based dielectrics, resulting in stable, clean and efficient discharging process and generation of a smoother surface²³. Also, lowest viscosity of distilled water with 10% ethanol dielectrics should encourage the occurrence of multi-discharging which leads to more distribution of discharging energy in discharging zone and consequently craters with shallower depths are created resulting in smoother surface topography. Also, in Distilled water mixed with 10% ethanol the expansion of bubbles is less restricted due to dielectric's extremely low viscosity and density. Accordingly, the pressure over the discharge zone could experience a much more fluctuation and faster expansion speeds of the bubbles. Therefore, least SR in 6 out of 9 cases was obtained from Distilled water with 10% ethanol dielectric.

It can be concluded that Biodiesel produced the highest MRR but the lowest TWR. Valaki and rathod³³ obtained similar results. Bio-fuel (distilled water blended with 10% ethanol) resulted in the lowest SR. Hence cleaner, greener and more environmentally friendlier as well as healthier solution of using bio-dielectrics such as biodiesel from waste cooking oil and bio-fuel (distilled water with 10% ethanol) for improving sustainability of EDM process passed successful trials for operational feasibility assessments as well.

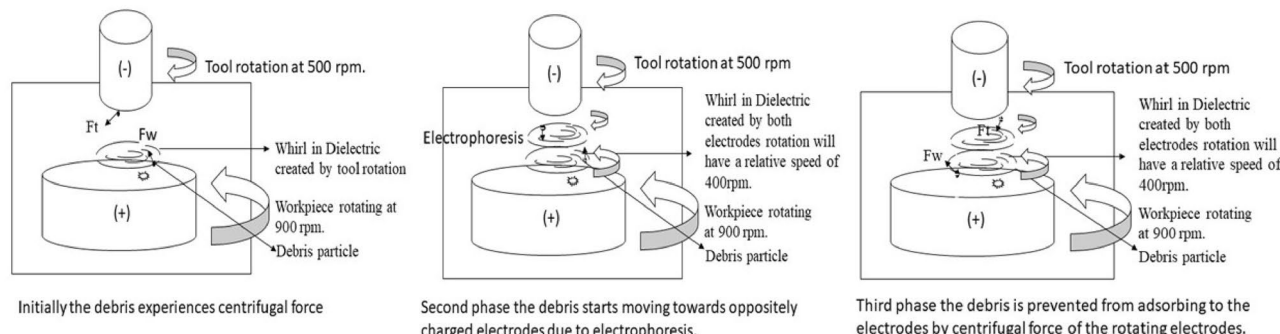


Fig. 37. Shows debris movement in case of opposite direction rotation of both electrodes.

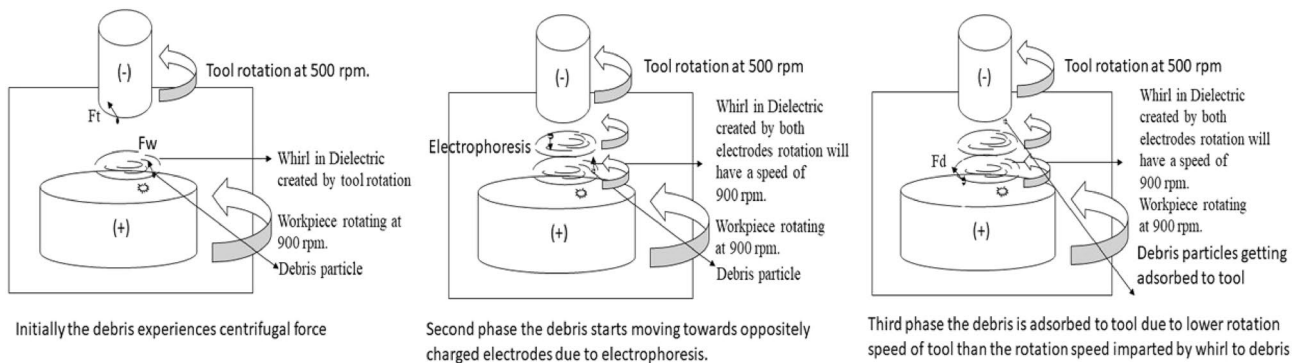


Fig. 38. Shows the debris movement in case of same direction rotation of both electrodes.

Both electrodes rotation

Table 6 shows that rotation of both electrodes contributed 3.71% to MRR and also significantly affected MRR. From main effect plot of signal to noise ratio for MRR Fig. 16 it was observed that opposite direction rotation of both electrodes gave most MRR followed by same direction rotation of both electrodes and no rotation of both electrodes. Table 6 shows that rotation of both electrodes contributed 3.46% to TWR. From main effect plot of signal to noise ratio for TWR Fig. 18 it was observed that no rotation of both electrodes produces least TWR followed by opposite direction rotation of both electrodes and same direction rotation of both electrodes. Table 6 shows that rotation of both electrodes contributed 38.30% to SR and also significantly affected the SR. From main effect plot of signal to noise ratio for SR Fig. 20 it was observed that opposite direction rotation of both electrodes produced least surface roughness followed by same direction and no rotation of both electrodes.

The simultaneous rotation of both electrodes in a dielectric environment creates a whirl effect⁶⁸. However, if the electrodes rotate in opposite directions, a whirl effect equivalent to the relative velocity of the both electrodes is produced. The rotation of tool and workpiece also generates centrifugal force on debris particles⁶⁹, causing them to be expelled from their respective electrodes. However since the debris particles are very small in size (185–199 nm)⁴² the centrifugal force acting on them will also be small. This debris behaves as colloidal particles in dielectric which acquires charge by adsorbing the dissociated ions. Hence the charged debris will move toward oppositely charged electrodes under the influence of electrophoresis. Since comparatively more debris is removed from workpieces, after initial outward throw, debris will move toward tool under electrophoresis having the motion same as the dielectric whirl⁷⁰. However, the opposite direction rotation of the tool prevents the adsorption of debris on the tool, due to centrifugal force generated. This prevents the adsorption of debris to the tool. Also, since workpiece rotation is 900 rpm which is larger than tool rotation i.e., 500 rpm hence the whirl in dielectric will in the direction of workpiece rotation. Opposite direction rotation of tool, will force the tool to drag against the dielectric whirl, thereby further removing debris accumulation on tool and creating a sort of self-cleaning of the tool. Any debris moving toward workpiece piece, will be thrown away by larger whirl force in the dielectric. The improved flushing of debris enhances the stability of the process and increases the number of normal discharges, resulting in a better spark and increased MRR and decreased TWR and SR. The same is demonstrated in the Fig. 37.

When both electrodes are rotated in the same direction, a whirl is created in the dielectric medium, which corresponds to the rotation of the workpiece electrode with a higher rpm. The debris generated by sparking, experiences an outward centrifugal force due to the rotation of the electrodes. However since the debris particles are very small in size (185–199 nm)⁴² the centrifugal force acting on them will also be small. This debris behaves as colloidal particles in the dielectric medium and gets charged by adsorbing dissociated ions. As a result, the charged debris moves towards the oppositely charged electrode, either the cathode or anode. Since more debris is removed from the workpiece, it initially moves outward but then moves towards the tool under electrophoresis, following the motion of the dielectric whirl⁷⁰.

Tool wear provides a larger space for debris accumulation⁷⁰, and rotating the tool in the same direction at lower speeds does not provide an outward force to the debris. Therefore, the debris is easily adsorbed onto the tool surface. Moreover, the drag of the tool against the whirl is equal to its relative velocity, resulting in less self-cleaning. Hence, less flushing occurs when both electrodes are rotated in the same direction with the tool rotation being smaller than the workpiece rotation, resulting in inadequate debris flushing, more short-circuiting, and arc discharge. Consequently, the MRR is lower, and the TWR and SR are higher than when both electrodes are rotated in opposite directions.

However, further experiments are required with a higher tool rotation than workpiece rotation to reject the same direction rotation of both electrodes' performance parameters in favour of opposite direction rotation. Figure 38 illustrates the above phenomenon.

Rotating both electrodes during the machining process can lead to improved surface finish due to the constant changing of the spark gap, resulting in a more evenly distributed electric discharge. In particular, the use of opposite direction rotation has been found to be more effective in providing a better surface finish compared to same direction rotation. This is attributed to the improved flushing of debris, which prevents remelting of debris during the next discharge and sticking onto the work surface⁶⁸. Additionally, opposite direction rotation provides new peaks for the tool to generate sparks at a faster relative speed, resulting in better distribution of

Both electrodes rotation direction	Tool treatment	Bio-dielectric	s/n ratio			Normalization			deviation sequence			Grey relational coefficient			Grade	rank
			MRR	TWR	SR	MRR	TWR	SR	MRR	TWR	SR	MRR	TWR	SR		
Opposite	HTT	Water-ethanol	29.899	7.799	-7.328	0.879	0.930	0.338	0.121	0.070	0.662	0.806	0.878	0.430	0.705	2
Opposite	NTT	EDM oil	26.643	16.767	-7.513	0.775	0.650	0.362	0.225	0.350	0.638	0.690	0.588	0.439	0.572	19
No rotation	CTT	Water-ethanol	18.916	7.462	-12.413	0.528	0.941	1.000	0.472	0.059	0.000	0.514	0.895	1.000	0.803	1
Same	CTT	Water-ethanol	26.604	8.250	-8.707	0.774	0.916	0.517	0.226	0.084	0.483	0.689	0.857	0.509	0.685	5
No rotation	HTT	Water-ethanol	2.415	17.187	-12.203	0.000	0.637	0.973	1.000	0.363	0.027	0.333	0.579	0.948	0.620	15
Same	HTT	Water-ethanol	26.357	8.913	-6.547	0.766	0.896	0.236	0.234	0.104	0.764	0.681	0.827	0.396	0.635	12
Same	HTT	EDM oil	23.217	8.106	-7.421	0.666	0.921	0.350	0.334	0.079	0.650	0.599	0.863	0.435	0.632	13
No rotation	NTT	EDM oil	29.658	25.001	-9.615	0.872	0.392	0.635	0.128	0.608	0.365	0.796	0.451	0.578	0.608	16
Opposite	HTT	EDM oil	29.464	15.899	-9.020	0.865	0.677	0.558	0.135	0.323	0.442	0.788	0.607	0.531	0.642	11
No rotation	HTT	Bio diesel	24.028	15.351	-6.848	0.692	0.694	0.275	0.308	0.306	0.725	0.618	0.620	0.408	0.549	21
Same	NTT	Water-ethanol	26.048	6.198	-7.235	0.756	0.981	0.325	0.244	0.019	0.675	0.672	0.963	0.426	0.687	4
Same	NTT	EDM oil	10.559	19.266	-7.140	0.261	0.571	0.313	0.739	0.429	0.687	0.403	0.538	0.421	0.454	27
Opposite	CTT	Bio diesel	24.017	23.606	-7.513	0.691	0.436	0.362	0.309	0.564	0.638	0.618	0.470	0.439	0.509	26
Opposite	CTT	EDM oil	26.721	16.439	-7.604	0.778	0.660	0.374	0.222	0.340	0.626	0.692	0.595	0.444	0.577	18
Same	NTT	Bio diesel	28.583	19.516	-10.436	0.837	0.564	0.742	0.163	0.436	0.258	0.754	0.534	0.660	0.649	10
No rotation	NTT	Water-ethanol	6.783	9.504	-11.364	0.140	0.877	0.863	0.860	0.123	0.137	0.368	0.803	0.785	0.652	9
No rotation	HTT	EDM oil	33.095	16.966	-8.131	0.982	0.643	0.442	0.018	0.357	0.558	0.965	0.584	0.473	0.674	7
No rotation	CTT	EDM oil	33.668	19.629	-8.045	1.000	0.560	0.431	0.000	0.440	0.569	1.000	0.532	0.468	0.667	8
Same	CTT	EDM oil	26.173	24.822	-7.604	0.760	0.398	0.374	0.240	0.602	0.626	0.676	0.454	0.444	0.524	25
Same	HTT	Bio diesel	27.235	18.091	-7.959	0.794	0.608	0.420	0.206	0.392	0.580	0.708	0.561	0.463	0.577	17
No rotation	NTT	Bio diesel	23.439	22.261	-9.686	0.673	0.478	0.645	0.327	0.522	0.355	0.604	0.489	0.585	0.559	20
Opposite	CTT	Water-ethanol	23.087	6.065	-8.787	0.661	0.985	0.528	0.339	0.015	0.472	0.596	0.970	0.514	0.694	3
Opposite	NTT	Water-ethanol	27.601	5.578	-4.736	0.806	1.000	0.000	0.194	0.000	1.000	0.720	1.000	0.333	0.685	6
Opposite	NTT	Bio diesel	30.533	37.520	-7.959	0.900	0.000	0.420	0.100	1.000	0.580	0.833	0.333	0.463	0.543	22
Opposite	HTT	Bio diesel	26.486	19.557	-6.749	0.770	0.562	0.262	0.230	0.438	0.738	0.685	0.533	0.404	0.541	23
No rotation	CTT	Bio diesel	23.355	20.508	-11.126	0.670	0.533	0.832	0.330	0.467	0.168	0.602	0.517	0.749	0.623	14
Same	CTT	Bio diesel	24.769	19.961	-7.604	0.715	0.550	0.374	0.285	0.450	0.626	0.637	0.526	0.444	0.536	24

Table 7. Shows grey relational analysis.

sparks and a more uniform surface finish. Furthermore, rotating both electrodes can also prevent the occurrence of cracks and other defects during the machining process, thereby maintaining the surface integrity. It also reduces electrically conductive residues which can cause contamination and affect accuracy of machining process. Hence it can be concluded that by rotating both electrodes, improved accuracy, efficiency, productivity and uniformity of the machined surface is obtained.

Copper tool treatment

Annealing the copper tool made the copper softer, more ductile, malleable and uniform in structure with increased grain size as shown in Table 3. The colour of the tool changed to blackish/ dark reddish due to the formation of copper oxide on the surface. Also, electrical conductivity is reduced. Cryogenically cooling the copper tool and then again heating it for 200°C for 2 h (tempering) made the tool. Further soft and more porous as heat causes the Cu to expand and creates microcracks on the surface as in Table 1. Cryogenic treatment also improves electrical and thermal conductivity of tool material⁷¹.

Table 6 indicated that the impact of tool treatment on MRR was minimal, accounting for only 1.26% of the total variation. In Fig. 16, the main effect plot for MRR (signal-to-noise ratio) revealed that cryogenically treated tools (CTT) exhibited the highest MRR, followed by heat-treated tools (HTT) and non-treated tools (NTT). This finding suggests that softer tools, such as CTT generated more MRR than harder tools like NTT, which is consistent with the results reported by Rahul et al.⁴⁸. Furthermore, T. Muthuramalingam and B. Mohan⁷² demonstrated that tools with higher electrical conductivity produced greater MRR due to the increased flow of charges. Cryogenic treatment enhances the electrical and thermal conductivity of tool materials⁷¹, leading to improved MRR performance. The application of cryogenically cooled tool electrodes^{47–49} has also yielded higher MRR results in literature also.

Table 6 reveals that the contribution of tool treatment towards TWR was found to be minimum, accounting for only 0.19%. The main effect plot for TWR, as depicted in Fig. 18 illustrates that the lowest TWR was observed in the case of NTT, followed by CTT and HTT, with NTT being the hardest tool. This is primarily due to the fact that the thermal conductivity of the tool has a direct impact on TWR, with higher thermal conductivity leading to higher TWR. Cryogenically cooled tool electrodes have been found to give reduced TWR^{47–49,73} in literature.

Cryogenic treatment leads to a significant improvement in the electrical and thermal conductivity of the tool material⁷¹, facilitating enhanced heat dissipation through the tool electrode and thereby reducing tool wear.

However, carbon debris production from decomposition of hydrocarbon-based dielectrics at high temperatures hinders the stable and efficient discharging process. Additionally, the carbon is deposited on the tool, which is more pronounced when no rotation is used. Hence TWR was small due to the carbon deposition on tool after EDM as well as dielectric absorption by the tool due to tool porosity.

Table 6 showed that tool treatment was the most contributing factor for SR (2.88%). From the main effect plot for SR (signal to noise ratio) Fig. 20 it was observed that lowest SR was obtained by HTT followed by NTT and CTT.

Interaction of process parameters

Figure 21 show that the interaction between dielectric and rotation of both electrodes, dielectric and tool treatment and rotation of both electrodes and tool treatment had combined effect on MRR. Table 6 shows that all the above interaction significantly affected MRR with dielectric and rotation of both electrodes contributing 58.28% followed by dielectric and tool treatment contributing 11.29% and rotation of both electrodes and tool treatment contributing 8.05% to MRR. Regarding biodiesel MRR was maximum for opposite direction rotation of both electrodes and non-treated tool. In EDM oil, maximum MRR was achieved by no rotation of both electrodes and cryogenic-treated copper tool. In Distilled water plus 10% ethanol maximum MRR was achieved by opposite direction rotation of both electrodes and Heat-treated copper tool. Similarly for cryogenic treated tool no rotation gave maximum MRR, Heat treated tool and non-treated tool opposite direction rotation of both electrodes gave maximum MRR.

Figure 22 show that the interaction between dielectric and rotation of both electrodes, dielectric and tool treatment and rotation of both electrodes and tool treatment had combined effect on TWR. Table 6 shows that only dielectric and tool treatment interaction significantly affected TWR with most (11.84%) contribution to TWR. Regarding biodiesel, non-treated tool gave least TWR, EDM oil cryogenic treated tool gave least TWR and Distilled water plus 10% ethanol Heat treated tool gave least TWR.

Figure 23 show that the interaction between dielectric and opposite/same direction rotation of both electrodes, dielectric and tool treatment and opposite/same direction rotation of both electrodes and tool treatment had combined effect on SR. Table 6 shows that only dielectric and rotation of both electrodes interaction significantly affected SR with most contribution (27.43%) to SR. Regarding biodiesel SR was least for opposite direction rotation of both electrodes. In EDM oil, least SR was achieved by same direction rotation of both electrodes. In Distilled water plus 10% ethanol least SR was achieved by opposite direction rotation of both electrodes.

Table 7 displays the calculated Grey relational grade (GRG) coefficient. It was discovered that distilled water plus 10% ethanol as dielectric, cryogenic treated copper tool and no rotation of both tool gave the highest grey relational grade for combined performance parameters.

Conclusion

To address the challenges of unsustainability, environmental pollution, and economic inefficiency in Electrical Discharge Machining (EDM), a sustainable approach was proposed. This involved the use of biodiesel and distilled water, along with 10% ethanol as a bio-dielectric. Furthermore, the performance of the EDM process was optimized by varying the rotation of both electrodes (i.e., same direction, opposite direction, and no rotation) and the use of treated tools (i.e., no treatment, heat treatment, and cryogenic treatment). The use of biodiesel as a bio-dielectric offers a promising solution to address the aforementioned challenges. Key results obtained can be summarized as

- (1) Biodiesel produced the highest MRR and lowest TWR.
- (2) Distilled water blended with 10% ethanol (Biofuel) resulted in the lowest SR.
- (3) Additionally, the study found that the use of electrode rotation improved flushing, leading to better performance parameters. The opposite direction rotation of both electrodes produced most MRR and least SR.
- (4) However, no rotation of both electrodes gave least TWR.
- (5) Furthermore, the use of treated tools, such as heat-treated or cryogenically treated tools, also improved performance parameters and resulted in lower energy consumption.
- (6) CTT gave most MRR, HTT gave least SR and NTT gave least TWR. Also, certain interactions also significantly affected the performance parameters.
- (7) Grey relational analysis showed that distilled water with 10% ethanol as dielectric, cryogenic treated copper tool and no rotation of both tools gave the best performance parameters.

Future work

To further optimize the performance parameters, it is necessary to investigate the effect of rotating both electrodes in the same direction, starting from zero relative speed to higher ones. Moreover, before concluding whether the same or opposite direction rotation of both electrodes provides better performance measures, it is essential to explore the impact of keeping tool rotation speeds higher than workpiece rotation for the same direction rotation of both electrodes.

Data availability

All data generated or analysed during this study are included in this published article.

Received: 26 March 2024; Accepted: 30 August 2024
Published online: 08 October 2024

References

1. Kuppan, P., Rajadurai, A. & Narayanan, S. Influence of EDM process parameters in deep hole drilling of Inconel 718. *Int. J. Adv. Manuf. Technol.* **38**, 74–84. <https://doi.org/10.1007/s00170-007-1084-y> (2008).
2. Singh, G. *et al.* Surface morphology and microhardness behavior of 316L in HAP-PMEDM. *FU Mech. Eng.* **17**, 445–454 (2019).
3. Abdul-Rani, A. M., Razak, M. A., Littlefair, G., Gibson, I. & Nanimina, A. M. Improving EDM process on AZ31 magnesium alloy towards sustainable biodegradable implant manufacturing. *Procedia Manuf.* **7**, 504–509. <https://doi.org/10.1016/j.promfg.2016.12.057> (2017).
4. Soni, J. & Chakraverti, G. Surface characteristics of titanium with rotary EDM. *Bull. Mater. Sci.* **16**(3), 213–227 (1993).
5. Khan, M. Y., Rao, P. S. & Pabla, B. S. An experimental study on magnetic field-assisted-EDM process for Inconel-625. *Adv. Mater. Process. Technol.* **8**(sup4), 2204–2230. <https://doi.org/10.1080/2374068X.2022.2036450> (2022).
6. Upadhyay, L., Aggarwal, M. L. & Pandey, P. M. Experimental investigations into rotary magnetic field and tool assisted electric discharge machining using magneto rheological fluid as dielectric. *Int. J. Mechatron. Manuf. Syst.* **12**(1), 1–19 (2019).
7. Lin, Y. C., Yan, B. H. & Chang, Y. S. Machining characteristics of titanium alloy (Ti-6Al-4V) using a combination process of EDM with USM. *J. Mater. Process. Technol.* **104**(3), 171–177. [https://doi.org/10.1016/S0924-0136\(00\)00539-2](https://doi.org/10.1016/S0924-0136(00)00539-2) (2000).
8. Ni, H., Gong, H., Dong, Y. H., Fang, F. Z. & Wang, Y. A comparative investigation on hybrid EDM for drilling small deep holes. *Int. J. Adv. Manuf. Technol.* **95**(1–4), 1465–1472. <https://doi.org/10.1007/s00170-017-1282-1> (2018).
9. Srivastava, V. & Pandey, P. M. Effect of process parameters on the performance of EDM process with ultrasonic assisted cryogenically cooled electrode. *J. Manuf. Process.* **14**(3), 393–402. <https://doi.org/10.1016/j.jmapro.2012.05.001> (2012).
10. Bains, P. S., Singh, S., Sidhu, S. S., Kaur, S. & Ablyaz, T. R. Investigation of surface properties of Al-SiC composites in hybrid electrical discharge machining. In *Futuristic Composites Behaviour, Characterization and Manufacturing* (ed. Bains, P. S.) (Springer, 2018). <https://doi.org/10.1007/978-981-13-2417-8>.
11. Ali, P., Qasim, R. S. W., Ranganath, M. & Singari, M. Material removal analysis of hybrid EDM—Assisted centrifugal abrasive flow machining process for performance enhancement. *J. Braz. Soc. Mech. Sci. Eng.* <https://doi.org/10.1007/s40430-020-02375-6> (2020).
12. Prakash, C., Singh, S., Yongling, L., Zheng, W. H. Y. & Królczyk, G. Functional grading of surfaces through hybrid ultrasonic, abrasive water jet, and electric discharge machining processing. *J. Braz. Soc. Mech. Sci. Eng.* **43**(4), 1–8. <https://doi.org/10.1007/s40430-021-02931-8> (2021).
13. Das, S., Paul, S. & Doloi, B. Feasibility assessment of some alternative dielectric mediums for sustainable electrical discharge machining: A review work. *J. Braz. Soc. Mech. Sci. Eng.* **42**(4), 1–21. <https://doi.org/10.1007/s40430-020-2238-1> (2020).
14. Li, G., Natsu, W. & Yu, Z. Study on quantitative estimation of bubble behavior in micro hole drilling with EDM. *Int. J. Mach. Tools Manuf.* **146**, 103437. <https://doi.org/10.1016/j.ijmachtools.2019.103437> (2019).
15. Bommeli, B. Study of the harmful emanations resulting from the machining by electro-erosion. (1983).
16. Jagadish, A. R. Multi-objective optimization of green EDM: An integrated theory. *J. Inst. Eng. (India) Ser. C* **96**(1), 41–47. <https://doi.org/10.1007/s40032-014-0142-0> (2015).
17. Mishra, B. P. & Routara, B. C. Evaluation of technical feasibility and environmental impact of Calophyllum Inophyllum (Polanga) oil based bio-dielectric fluid for green EDM. *Measurement* **159**, 107744. <https://doi.org/10.1016/j.measurement.2020.107744> (2020).
18. M. Dastagiri, P. S. Rao, and P. M. Valli, Feasibility of Reused Palm oil Blends as a Dielectric Medium for Electric Discharge Machine. *Int. J. Innov. Technol. Explor. Eng.* (2019).
19. Basha, S. M., Dave, H. K. & Patel, H. V. Materials Today : Proceedings Experimental investigation of jatropha curcas bio-oil and biodiesel in electric discharge machining of Ti-6Al-4V. *Mater. Today Proc.* <https://doi.org/10.1016/j.matpr.2020.04.536> (2020).
20. Valaki, J. B., Rathod, P. P. & Sankhavara, C. D. Investigations on technical feasibility of Jatropha curcas oil based bio dielectric fluid for sustainable electric discharge machining (EDM). *J. Manuf. Process.* **22**, 151–160. <https://doi.org/10.1016/j.jmapro.2016.03.004> (2016).
21. Singaravel, B., Shekar, K. C., Reddy, G. G. & Prasad, S. D. Experimental investigation of vegetable oil as dielectric fluid in Electric discharge machining of Ti-6Al-4V. *Ain Shams Eng. J.* <https://doi.org/10.1016/j.asej.2019.07.010> (2019).
22. Tang, L. & Du, Y. T. Experimental study on green electrical discharge machining in tap water of Ti-6Al-4V and parameters optimization. *Int. J. Adv. Manuf. Technol.* **70**(1–4), 469–475. <https://doi.org/10.1007/s00170-013-5274-5> (2014).
23. Das, S., Paul, S. & Doloi, B. Assessment of the impacts of bio-dielectrics on the textural features and recast-layers of EDM- surfaces. *Mater. Manuf. Process.* **00**(00), 1–11. <https://doi.org/10.1080/10426914.2020.1832678> (2020).
24. S. Das, S. Paul, and B. Doloi, Feasibility investigation of neem oil as a dielectric for electrical discharge machining. *Int. J. Adv. Manuf. Technol.* pp. 1179–1189, (2020).
25. Dhakar, K. & Dvivedi, A. ScienceDirect experimental investigation on near-dry EDM using glycerin-air mixture as dielectric medium. *Mater. Today Proc.* **4**(4), 5344–5350. <https://doi.org/10.1016/j.matpr.2017.05.045> (2017).
26. J. B. Valaki, P. P. Rathod, B. C. Khatri, and J. R. Vaghela, Investigations on palm oil based biodielectric fluid for sustainable electric discharge machining. In: *International Conference on Advances in Materials and Manufacturing (ICAMM-2016)*, 2016, (2018).
27. Bajaj, R., Rai, A., Arun, D. & Tiwari, K. Machining performance enhancement of powder mixed electric discharge machining using Green dielectric fluid. *J. Braz. Soc. Mech. Sci. Eng.* <https://doi.org/10.1007/s40430-020-02597-8> (2020).
28. Reddy, G. G., Singaravel, B. & Shekar, K. C. Experimental investigation of sunflower oil as dielectric fluid in die sinking electric discharge machining process. *Mater. Sci. Forum* **969**, 715–719. <https://doi.org/10.4028/www.scientific.net/MSF.969.715> (2019).
29. Radhakrishnan, R. Multi-response optimization of process parameters of green electrical discharge machining on aisi 2507 super duplex stainless steel using grey relational analysis (Gra). *Int. J. Mech. Prod. Eng. Res. Dev.* (2018).
30. Das, S., Paul, S. & Doloi, B. An experimental and computational study on the feasibility of bio-dielectrics for sustainable electrical discharge machining. *J. Manuf. Process.* **41**(March), 284–296. <https://doi.org/10.1016/j.jmapro.2019.04.005> (2019).
31. Singh, N. K., Yadav, L. & Lal, S. Experimental investigation for sustainable electric discharge machining with Pongamia and Jatropha as dielectric medium. *Adv. Mater. Process. Technol.* **00**(00), 1–20. <https://doi.org/10.1080/2374068X.2020.1860499> (2020).
32. Khan, M. I., Chhetri, A. B. & Islam, M. R. Analyzing sustainability of community-based energy technologies. *Energy Sources B* <https://doi.org/10.1080/15567240600814896> (2007).
33. Valaki, J. B. & Rathod, P. P. Assessment of operational feasibility of waste vegetable oil based bio-dielectric fluid for sustainable electric discharge machining (EDM). *Int. J. Adv. Manuf. Technol.* <https://doi.org/10.1007/s00170-015-7169-0> (2015).
34. Chen, S. L., Yan, B. H. & Huang, F. Y. Influence of kerosene and distilled water as dielectrics on the electric discharge machining characteristics of Ti – 6A1 – 4V. *J. Mater. Process. Technol.* **87**, 107–111 (1999).
35. G. Dunnebacke, High performance electrical discharge machining using a water-based dielectric. In: *Proc. 10th International Symposium for Electro machining (ISEM X)*. pp. 170–182.
36. Masuzawa, T., Tanaka, K. & Nakamura, Y. Water-based dielectric solution for EDM. *CIRP Ann.* **32**(1), 119–122. [https://doi.org/10.1016/s0007-8506\(07\)63374-5](https://doi.org/10.1016/s0007-8506(07)63374-5) (1983).
37. Konig, W. & Jorres, L. Aqueous solutions of organic compounds as dielectrics for EDM sinking. *Ann. CIRP* **36**, 105–109 (1987).

38. Yan, B. H., Tsai, H. C. & Huang, F. Y. The effect in EDM of a dielectric of a urea solution in water on modifying the surface of titanium. *Int. J. Mach. Tools Manuf.* **45**, 194–200. <https://doi.org/10.1016/ijmachtools.2004.07.006> (2005).
39. Goldemberg, Å., Coelho, S. T. & Guardabassi, P. The sustainability of ethanol production from sugarcane. *Energy Policy* **36**, 2086–2097. <https://doi.org/10.1016/j.enpol.2008.02.028> (2008).
40. R. M. Rakesh Sarwal, Sunil Kumar, Amit Mehta, Amit Varadan, Subodh Kumar Singh, S.S.V Ramakumar, *Road map for ETHANOL BLENDING IN INDIA 2020–25, Niti Aayog, Ministry of petroleum and Natural Gas.* (2020).
41. Tsiropoulos, I., Faaij, A. P. C. & Seabra, J. E. A. Life cycle assessment of sugarcane ethanol production in India in comparison to Brazil. *Int. J. Life Cycle Assess.* <https://doi.org/10.1007/s11367-014-0714-5> (2014).
42. Shabgard, M. R. & Kabirinia, F. Effect of dielectric liquid on characteristics of WC-Co powder synthesized using EDM process. *Mater. Manuf. Process.* **29**, 1269–1276. <https://doi.org/10.1080/10426914.2013.852207> (2014).
43. Gonzalez, B., Calvar, N., Go, E. & Dominguez, A. Density, dynamic viscosity, and derived properties of binary mixtures of methanol or ethanol with water, ethyl acetate, and methyl acetate at $T = (293.15, 298.15, \text{ and } 303.15) \text{ K}$. *J. Chem. Thermodyn.* **39**, 1578–1588. <https://doi.org/10.1016/j.jct.2007.05.004> (2007).
44. T. Gutowski, J. Dahmus, and A. Thiriez, “Electrical Energy Requirements for Manufacturing Processes 生产过程的电能要求,” *13th CIRP INTERNATIONAL CONFERENCE ON LIFE CYCLE ENGINEERING*, pp. 623–628 (2006).
45. Wang, C. C. & Yan, B. H. Blind-hole drilling of Al2O3/6061Al composite using rotary electro-discharge machining. *J. Mater. Process. Technol.* **102**(1), 90–102. [https://doi.org/10.1016/S0924-0136\(99\)00423-9](https://doi.org/10.1016/S0924-0136(99)00423-9) (2000).
46. U. Arif, imtiaz ali Khan, and F. Hasan, Investigating the effect of novel ushering parameters in RT-RW-EDM of Al-SiCmicro-SiC nano hybrid composite using ANN and PSO. <https://doi.org/10.21203/rs.3.rs-3726980/v1> (2024).
47. Hui, Z., Liu, Z., Cao, Z. & Qiu, M. Effect of cryogenic cooling of tool electrode on machining titanium alloy (Ti-6Al-4V) during EDM. *Mater. Manuf. Process.* **31**(4), 475–482. <https://doi.org/10.1080/10426914.2015.1037893> (2016).
48. Rahul, D. K., Mishra, S., Datta, and M. Masanta, Effects of Tool Electrode on EDM Performance of Ti-6Al-4V. *Silicon* **10**(5), 2263–2277. <https://doi.org/10.1007/s12633-018-9760-0> (2018).
49. Cetin, A. C. A., Cakir, G., Alsanitas, K. & Ucak, N. Performance of cryogenically treated Cu and CuCrZr electrodes in an EDM process. *Kovacs Mater.* **55**, 431–440. <https://doi.org/10.4149/km20176431> (2017).
50. Rahul, S., Datta, B., Bhushan, and S. Sankar, Electrical discharge machining of Inconel 825 using cryogenically treated copper electrode: Emphasis on surface integrity and metallurgical characteristics. *J. Manuf. Process.* **26**, 188–202. <https://doi.org/10.1016/j.jmapro.2017.02.020> (2017).
51. Shabgard, M., Rezaei, M. & Hossein, Z. Experimental investigation on the effect of SiC particles in machining process of Al—5.3% CU—SiC p—Al 2 O 3p hybrid nanocomposite by EDM. *SN Appl. Sci.* **1**(5), 1–9. <https://doi.org/10.1007/s42452-019-0401-z> (2019).
52. Shukla, M., Agarwal, P., Pradhan, M. K. & Dhakad, S. K. Experimental investigation of EDM parameters on Al-LM6/SiC/B4C hybrid experimental investigation of EDM parameters on Al-LM6/SiC/B4C hybrid composites. *Appl. Mech. Mater.* **877**(February), 149–156. <https://doi.org/10.4028/www.scientific.net/AMM.877.149>.
53. Senthilkumar, T. S. & Muralikannan, R. Enhancing the geometric tolerance of aluminium hybrid metal matrix composite using EDM process. *J. Braz. Soc. Mech. Sci. Eng.* <https://doi.org/10.1007/s40430-018-1553-2> (2019).
54. Ramaswamy, A. & Perumal, A. V. Multi - objective optimization of drilling EDM process parameters of LM13 Al alloy—10ZrB 2–5TiC hybrid composite using RSM. *J. Braz. Soc. Mech. Sci. Eng.* **42**(8), 1–18. <https://doi.org/10.1007/s40430-020-02518-9> (2020).
55. Ponappa, K., Sasikumar, K. S. K., Sambathkumar, M. & Udhayakumar, M. Multi objective optimization of EDM process parameters for machining of hybrid aluminum metal matrix composites (Al7075/ TiC/B4C) using genetic algorithm. *Surf. Rev. Lett.* <https://doi.org/10.1142/S0218625X19500719> (2018).
56. Radhika, N., Addamane, S. & Chandran, G. K. Optimization of electrical discharge machining parameters of aluminium hybrid composites using Taguchi method. *J. Eng. Sci. Technol.* **9**, 502–512 (2014).
57. Devi, M. B., Sameer, M. D. & Birru, A. K. EDM machining characteristics of bamboo leaf ash and alumina reinforced aluminum hybrid metal matrix composite using Multi-response optimization by grey relational analysis. *Mater. Res. Express* <https://doi.org/10.1088/2053-1591/ab824> (2021).
58. Özerkan, H. B., Subaşı, M. & Pul, M. Investigation of the machinability of B4C+TiB2/Al 2024 composite manufactured by powder metallurgy with EDM. *Proc. Inst. Mech. Eng. C J. Mech. Eng. Sci.* **237**(6), 1357–1369. <https://doi.org/10.1177/09544062221130219> (2023).
59. Matharou, G. S. & Bhuyan, B. K. Parametric optimization of edm processes for aluminum hybrid metal matrix composite using gra-pca approach. *Int. J. Mech. Prod. Eng. Res. Dev.* **10**(3), 367–378 (2020).
60. Yunus, M., Rao, P. S., Pabla, B. S. & Kumar, K. A. Feasibility of used cooking oil-based biodiesel (UCOB) as a dielectric for electrical discharge machining. *J. King Saud Univ. Sci.* **34**(8), 102305. <https://doi.org/10.1016/j.jksus.2022.102305> (2022).
61. Arif, U., Ali Khan, I. & Hasan, F. Thermal modeling and parametric optimization for machining of aluminum (Al-10%SiC micro -SiC nano)-based hybrid composite using spark erosion. *J. Mater. Eng. Perform.* <https://doi.org/10.1007/s11665-023-09042-6> (2023).
62. Umar, M. *et al.* Surface generation on titanium alloy through powder—Mixed electric discharge machining with the focus on bioimplant applications. *Int. J. Adv. Manuf. Technol.* <https://doi.org/10.1007/s00170-022-09927-1> (2022).
63. Asif, N., Saleem, M. Q. & Farooq, M. U. Performance evaluation of surfactant mixed dielectric and process optimization for electrical discharge machining of titanium alloy Ti6Al4V. *CIRP J. Manuf. Sci. Technol.* **43**, 42–56. <https://doi.org/10.1016/j.cirpj.2023.02.007> (2023).
64. K. Ishfaq and M. U. Farooq, Reducing the geometrical machining errors incurred during die repair and maintenance through electric discharge machining (EDM). pp. 3153–3168, (2021).
65. Farooq, M. U. *et al.* A novel flushing mechanism to minimize roughness and dimensional errors during wire electric discharge machining of complex profiles on Inconel. *Materials* <https://doi.org/10.3390/ma15207330> (2022).
66. Kumar, K., Singh, V., Katyal, P. & Sharma, N. EDM μ -drilling in Ti-6Al-7Nb: Experimental investigation and optimization using NSGA-II. *Int. J. Adv. Manuf. Technol.* **104**, 2727–2738 (2019).
67. Paul, T. R., Saha, A., Dey, V. & Majumder, H. Multi - objective optimization of some correlated process parameters in EDM of Inconel 800 using a hybrid approach. *J. Braz. Soc. Mech. Sci. Eng.* **41**(7), 1–11. <https://doi.org/10.1007/s40430-019-1805-9> (2019).
68. Teimouri, R. & Baseri, H. Experimental study of rotary magnetic field-assisted dry EDM with ultrasonic vibration of workpiece. *Int. J. Adv. Manuf. Technol.* **67**(5–8), 1371–1384. <https://doi.org/10.1007/s00170-012-4573-6> (2013).
69. Yadav, V. K., Singh, R., Kumar, P. & Dwivedi, A. Performance enhancement of rotary tool near-dry EDM process through tool modification. *J. Braz. Soc. Mech. Sci. Eng.* **43**(2), 1–16. <https://doi.org/10.1007/s40430-021-02806-y> (2021).
70. Li, G., Natsu, W. & Yu, Z. Elucidation of the mechanism of the deteriorating interelectrode environment in micro EDM drilling. *Int. J. Mach. Tools Manuf.* **167**, 103747. <https://doi.org/10.1016/j.ijmachtools.2021.103747> (2021).
71. Kalsi, N. S. *et al.* Cryogenic treatment of tool materials : A review. *Mater. Manuf. Process.* <https://doi.org/10.1080/10426911003720862> (2010).
72. Muthuramalingam, T. & Mohan, B. Influence of tool electrode properties on machinability in spark erosion machining. *Mater. Manuf. Process.* **28**(8), 939–943. <https://doi.org/10.1080/10426914.2013.763973> (2013).

73. Sana, M., Asad, M., Umar, M., Saqib, F. & Muhammad, A. Machine learning for multi—Dimensional performance optimization and predictive modelling of nanopowder—Mixed electric discharge machining (EDM). *Int. J. Adv. Manuf. Technol.* **130**(11), 5641–5664. <https://doi.org/10.1007/s00170-024-13023-x> (2024).

Author contributions

Umair Arif, Imtiaz Ali khan and Faisal hasan have contributed to the study conception and design. Umair Arif has contributed to writing, experiment conduction and data curation. Imtiaz Ali khan and Faisal hasan have read and approved the final manuscript.

Competing interests

The authors declare no competing interests.

Ethical approval

All authors have adhered to accepted ethical standards for genuine research.

Consent to publish

All authors have given their consent to publish.

Additional information

Correspondence and requests for materials should be addressed to U.A.

Reprints and permissions information is available at www.nature.com/reprints.

Publisher's note Springer Nature remains neutral with regard to jurisdictional claims in published maps and institutional affiliations.

Open Access This article is licensed under a Creative Commons Attribution-NonCommercial-NoDerivatives 4.0 International License, which permits any non-commercial use, sharing, distribution and reproduction in any medium or format, as long as you give appropriate credit to the original author(s) and the source, provide a link to the Creative Commons licence, and indicate if you modified the licensed material. You do not have permission under this licence to share adapted material derived from this article or parts of it. The images or other third party material in this article are included in the article's Creative Commons licence, unless indicated otherwise in a credit line to the material. If material is not included in the article's Creative Commons licence and your intended use is not permitted by statutory regulation or exceeds the permitted use, you will need to obtain permission directly from the copyright holder. To view a copy of this licence, visit <http://creativecommons.org/licenses/by-nc-nd/4.0/>.

© The Author(s) 2024